
Article:
Powley, HR, Krom, MD orcid.org/0000-0003-3386-9215 and Van Cappellen, P (2017) Understanding the unique biogeochemistry of the Mediterranean Sea: Insights from a coupled phosphorus and nitrogen model. Global Biogeochemical Cycles, 31 (6). pp. 1010-1031. ISSN 0886-6236

https://doi.org/10.1002/2017GB005648

AGU PUBLICATIONS

Global Biogeochemical Cycles

RESEARCH ARTICLE
10.1002/2017GB005648

Key Points:
- A biogeochemical phosphorus (P) and nitrogen (N) model explains nutrient distributions and trophic conditions in the Mediterranean Sea (MS)
- Large fractions of new production in the MS are supported by lateral inputs of marine inorganic and organic P, similar to subtropical gyres
- Differences in N:P ratios of inputs are mainly responsible for the differences in deepwater NO_3:PO_4 ratios of the Western and Eastern MS

Supporting Information:
- Supporting Information S1

Correspondence to:
H. R. Powley,
hrpowley@uwaterloo.ca

Citation:
Powley, H. R., M. D. Krom, and P. Van Cappellen (2017), Understanding the unique biogeochemistry of the Mediterranean Sea: Insights from a coupled phosphorus and nitrogen model, *Global Biogeochem. Cycles*, *31*, 1010–1031, doi:10.1002/2017GB005648.

Received 20 FEB 2017
Accepted 16 MAY 2017
Accepted article online 20 MAY 2017
Published online 29 JUN 2017

Understanding the unique biogeochemistry of the Mediterranean Sea: Insights from a coupled phosphorus and nitrogen model

Helen R. Powley[1], Michael D. Krom[1,2,3], and Philippe Van Cappellen[1]

[1]Ecohydrology Research Group, Water Institute and Department of Earth and Environmental Sciences, University of Waterloo, Waterloo, Ontario, Canada, [2]School of Earth and Environment, University of Leeds, Leeds, UK, [3]Department of Marine Biology, Charney School of Marine Sciences, University of Haifa, Haifa, Israel

Abstract The Mediterranean Sea (MS) is an oligotrophic basin whose offshore water column exhibits low dissolved inorganic phosphorus (P) and nitrogen (N) concentrations, unusually high nitrate (NO_3) to phosphate (PO_4) ratios, and distinct biogeochemical differences between the Western Mediterranean Sea (WMS) and Eastern Mediterranean Sea (EMS). A new mass balance model of P and N cycling in the WMS is coupled to a pre-existing EMS model to understand these biogeochemical features. Estimated land-derived inputs of reactive P and N to the WMS and EMS are similar per unit surface area, but marine inputs are 4 to 5 times greater for the WMS, which helps explain the approximately 3 times higher primary productivity of the WMS. The lateral inputs of marine sourced inorganic and organic P support significant fractions of new production in the WMS and EMS, similar to subtropical gyres. The mass balance calculations imply that the MS is net heterotrophic: dissolved organic P and N entering the WMS and EMS, primarily via the Straits of Gibraltar and Sicily, are mineralized to PO_4 and NO_3 and subsequently exported out of the basin by the prevailing anti-estuarine circulation. The high deepwater (DW) molar NO_3:PO_4 ratios reflect the high reactive N:P ratio of inputs to the WMS and EMS, combined with low denitrification rates. The lower DW NO_3:PO_4 ratio of the WMS (21) compared to the EMS (28) reflects lower reactive N:P ratios of inputs to the WMS, including the relatively low N:P ratio of Atlantic surface water flowing into the WMS.

Plain Language Summary The Mediterranean Sea (MS) is a marine desert: it exhibits extremely low biological productivity despite being almost entirely surrounded by land with high nutrient loadings from a large coastal population. To explain this paradox, we analyze the sources and fate of the two main nutrient elements that support the production of marine biomass, phosphorus (P), and nitrogen (N). We find that the main source of P and N to the MS is inflow of surface water from the Atlantic Ocean via the Strait of Gibraltar, not land-derived sources. This inflow is balanced by a return to the Atlantic Ocean of deeper Mediterranean water enriched in the biologically most active forms of P and N, phosphate and nitrate. The very low productivity of the MS therefore reflects a switch from less bioavailable chemical forms of P and N entering the MS to more bioavailable forms leaving the MS. Computer simulations reproduce these chemical differences when coupling the biological utilization and recycling of P and N to the circulation of the MS, which drives the water exchanges across the Strait of Gibraltar. These simulations also reproduce the differences in productivity and nutrient distributions between the western and eastern basins of the MS.

1. Introduction

The Mediterranean Sea (MS) is a major inland basin connected to the North Atlantic via the Strait of Gibraltar. It is oligotrophic, despite relatively high inputs of the essential nutrients phosphorus (P) and nitrogen (N) [*Béthoux et al.*, 2005; *Ludwig et al.*, 2009; *Powley et al.*, 2014, 2016a]. This apparent contradiction is ascribed to the unusual anti-estuarine circulation [*Krom et al.*, 2010] driven by excess evaporation within the basin [*Béthoux*, 1980]. Atlantic surface water (ASW) with relatively low inorganic P and N concentrations enters the Western Mediterranean Sea (WMS) through the Strait of Gibraltar, while deeper waters enriched in the inorganic nutrients are returned to the Atlantic Ocean. A similar exchange occurs between the WMS and the Eastern Mediterranean Sea (EMS) via the Strait of Sicily, a narrow passageway between Europe and Africa with a water depth of 360–430 m.

The two major basins of the MS, the WMS and EMS, have distinct biogeochemical properties. Deepwater (DW) phosphate (PO_4) and nitrate (NO_3) concentrations are approximately twice as high in the WMS compared to

the EMS [*Moutin and Raimbault*, 2002; *Pujo-Pay et al.*, 2011], while primary productivity is 2.5–3.3 times greater in the WMS than the EMS [*Turley et al.*, 2000; *Berman-Frank and Rahav*, 2012]. The differences in inorganic P and N concentrations and trophic conditions between the WMS and EMS appear to originate with differences in nutrient loading to the two basins and are subsequently maintained by the biological pump [*Crispi et al.*, 2001].

The EMS is the largest body of water that is unequivocally P limited [*Krom et al.*, 1991]. The winter phytoplankton bloom consumes all the dissolved phosphate within the surface water (SW), while measurable nitrate persists [*Krom et al.*, 1992]. In addition to the phytoplankton, bacteria in the EMS have also been shown to be strongly P limited [*Zohary and Robarts*, 1998]. Under summer conditions, bacteria and micrograzers in the EMS are P limited, while autotrophs tend to be P and N colimited [*Thingstad et al.*, 2005]. The situation in the WMS is not as clear-cut. The spring phytoplankton bloom has been proposed to be N limited [*Marty et al.*, 2002] or N and P colimited [*Pasqueron de Fommervault et al.*, 2015], while P limitation has been reported for the Gulf of Lions [*Diaz et al.*, 2001]. *Pasqueron de Fommervault et al.* [2015] argue that the dissolved inorganic N:P ratio of SW below 20:1 implies that there are periods of N limitation and periods of P limitation during the phytoplankton bloom, rather than only N limitation [*Marty et al.*, 2002]. During the summer stratification period in the WMS, P limitation generally occurs for both phytoplankton and heterotrophic bacteria [*Thingstad and Rassoulzadegan*, 1995; *Thingstad et al.*, 1998; *Marty et al.*, 2002; *Van Wambeke et al.*, 2002; *Pinhassi et al.*, 2006; *Pasqueron de Fommervault et al.*, 2015]. Model results further indicate that on an annual basis, P is the ultimate limiting nutrient for phytoplankton growth throughout the MS [*Lazzari et al.*, 2016].

There is a general consensus that the global ocean as a whole is autotrophic: it is responsible for about half the net productivity of the biosphere [*Falkowski et al.*, 2000], which in turn supports annual fish catches of 9.6×10^7 t [*Duarte et al.*, 2009]. Marine productivity, however, is not evenly distributed, with coastal areas and upwelling areas exhibiting particularly high productivity. In addition, it has been suggested that oligotrophic areas of the ocean are net heterotrophic [*Duarte et al.*, 2013] though this conclusion has been challenged [*Williams et al.*, 2013]. The MS offers an unusual situation. As an inland sea, it receives large external inputs of non-marine P and N, which would favor autotrophy. Formation of intermediate and deep waters in the MS, and their ultimate export to the Atlantic Ocean, however, maintains ultraoligotrophic conditions. At present, whether the MS is net autotrophic or heterotrophic remains an open question.

The molar NO_3:PO_4 DW ratios of the MS are especially high compared to the global ocean, increasing from 20–23:1 on average in the WMS to 26–30:1 within the EMS [*Krom et al.*, 1991; *Béthoux et al.*, 1998; *Kress and Herut*, 2001; *Moutin and Raimbault*, 2002; *Ribera d'Alcalà et al.*, 2003; *Schroeder et al.*, 2010; *Pujo-Pay et al.*, 2011]. Recent analyses suggest that for the EMS, the high N:P ratio of the external inputs, together with very limited denitrification [*Krom et al.*, 2010; *Huertas et al.*, 2012; *Van Cappellen et al.*, 2014], explains the very high NO_3:PO_4 DW ratios. The same may be true for the WMS [*Huertas et al.*, 2012] although N_2 fixation has also been invoked to explain the unusual high DW NO_3:PO_4 ratio [*Béthoux et al.*, 1992, 2002].

Existing biogeochemical models of the MS [e.g., *Crispi et al.*, 2001; *Allen et al.*, 2002; *Lazzari et al.*, 2012; *Macias et al.*, 2014; *Lazzari et al.*, 2016] focus on biological processes in the upper water column and the resulting ecosystem responses on seasonal timescales. Few models address the longer-term changes (i.e., $\geq$1 year) of the coupled P and N cycles across the entire MS, including the DW reservoirs. A biogeochemical mass balance model of P and N cycling in the EMS (excluding the Adriatic and Aegean Seas) was recently developed and applied to the second half of the twentieth century (1950–2000) [*Powley et al.*, 2014; *Van Cappellen et al.*, 2014]. The model incorporates the most up-to-date conceptual understanding of the key biogeochemical processes controlling the fate of P and N in the EMS, coupled to a simplified representation of the water cycle across the basin. The EMS model accounts for both inorganic and organic forms of P and N, as well as the temporal trajectories of P and N inputs and outputs.

Here we build on our previous work by developing a mass balance model for the P and N cycles in the WMS and then coupling it to the existing EMS model. The resulting WMS-EMS model is used to interpret the unusual biogeochemical features of the MS and, in particular, the differences in productivity and P and N distributions between the WMS and EMS. We also analyze whether the MS is net autotrophic or net heterotrophic. The conclusions presented in this paper rely on the reconstructed P and N cycles for the year 1950, that is, before the large increases in anthropogenic P and N inputs to the MS that took place during the second

half of the twentieth century [*Powley et al.*, 2014]. The effects of post-1950 changes in P and N inputs on primary productivity and water column nutrient concentrations of the MS are addressed in a companion paper.

2. Mass Balance Model

2.1. Circulation

Basin-scale circulation is represented using the water cycle model of *Powley et al.* [2016b]. Briefly, the WMS and EMS are both divided into three horizontal layers: surface water (WMSW and EMSW), intermediate water (WMIW and EMIW), and deep water (WMDW and EMDW) (Figure 1). The water cycle model accounts for the bidirectional flows across the Straits of Gibraltar and Sicily, as well as DW formation and upwelling in both the WMS and EMS. In the EMS, DW formation occurs in the Adriatic and Aegean Seas, which are separated from the Levantine and Ionian Basins by the Otranto and Cretan Straits, respectively. The Adriatic and Aegean Seas are excluded from the EMS model domain; that is, DW formation is modeled by imposing the water flux entering the EMDW. In the WMS, open-ocean DW formation originates near the Gulf of Lions in the northwestern part of the WMS. The corresponding area of about 25,000 km^2 falls outside the model domain; throughout this paper we will refer to this area as the north-west Mediterranean (NWM). The water cycle is assumed to be at steady state: annual flows in and out of each of the water reservoirs balance each other. A complete description of the water cycle can be found in *Powley et al.* [2016b]. Note that the estimated water residence time of 44 years for WMDW is approximately 3 times lower than that of 150 years for EMDW (Figure 1) [*Powley et al.*, 2016b].

2.2. Phosphorus and Nitrogen Cycling in the WMS

The WMS P and N concentrations and fluxes are assigned following the same approach used for the EMS by *Van Cappellen et al.* [2014]. Key model assumptions are as follows:

1. The annually integrated primary production in the WMS is P limited, and N assimilation is coupled to P uptake through the Redfield ratio (N:P = 16:1 [*Redfield et al.*, 1963]).
2. Prior to 1950, anthropogenic pressures on P and N cycling in the offshore waters of the WMS were relatively minor; hence, the P and N cycles in 1950 are assumed to be at steady state.

Phosphorus limitation of primary production is clearly established for the EMS, less so for the WMS. In fact, the Alboran Sea is probably N limited [*Ramirez et al.*, 2005; *Lazzari et al.*, 2016]. However, at the scale of the entire WMS basin, annual primary production is still primarily P, rather than N, limited. The phytoplankton bloom in the WMS is typically initiated by mixing of the water column, which brings NO_3-enriched water (i.e., with NO_3:$PO_4 > 16$) into the photic zone [*Severin et al.*, 2014], suggesting that P is the ultimate limiting nutrient. *Lazzari et al.* [2016] further conclude that on an annual basis the WMS is P limited based on their model simulations in which a variable intracellular N:P quota controls nutrient uptake by phytoplankton.

In most of the open ocean, the average, whole-phytoplankton community NO_3:PO_4 uptake ratio closely follows the Redfield value of N:P = 16 [*Klausmeier et al.*, 2004; *Arrigo*, 2005], although instantaneous ratios within and among different phytoplankton species may vary substantially (between 6:1 and 45:1 [*Geider and La Roche*, 2002; *Klausmeier et al.*, 2004]) Particularly in P-limited systems, such as the MS, the uptake ratio may exceed the Redfield value. For instance, for the EMS, *Krom et al.* [2014] report values of 16–25:1. In the absence of more definitive data, we impose the standard 16:1 Redfield value to calculate N assimilation in both WMSW and EMSW. To assess the sensitivity of the model predictions to the selected NO_3:PO_4 uptake ratio, we also performed a set of simulations with a NO_3:PO_4 uptake ratio of 23:1, a value that may be more representative of P-starved marine ecosystems [*Klausmeier et al.*, 2004]. The results are discussed in section 2.8.

The P reservoirs included in the model are dissolved inorganic P (PO_4), particulate organic P (POP), and dissolved organic P (DOP). The N reservoirs are dissolved nitrate plus nitrite (NO_3), dissolved ammonium (NH_4), particulate organic N (PON), and dissolved organic N (DON). All of the P and N reservoirs are represented in each of the water layers, resulting in a total of 9 P and 12 N reservoirs in the WMS model or 18 P and 24 N reservoirs in the combined WMS-EMS model. Throughout this paper total P (TP) encompasses both dissolved and particulate pools of P; that is, TP is the sum of PO_4, POP, DOP, and particulate inorganic P (PIP). Reactive P is defined as the sum of PO_4, POP, DOP, and for non-marine inputs to the MS, also the fraction of PIP that is

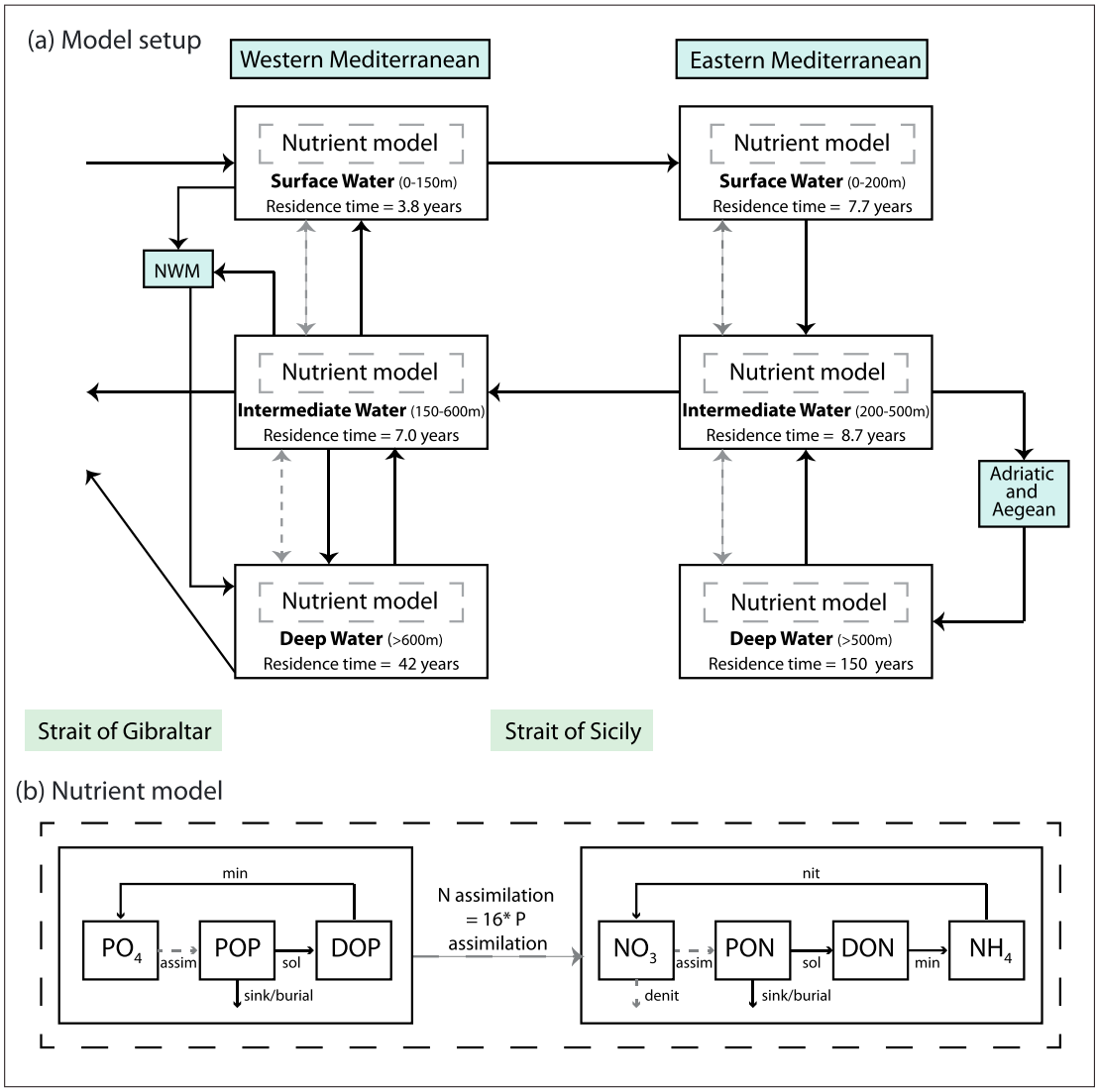

Figure 1. Conceptual model framework. (a) Water reservoirs and circulation: the black arrows represent advective water fluxes, the gray-dashed arrows represent turbulent mixing fluxes, and the water residence times are given for all reservoirs. Water fluxes and residence times are the same as those given in *Powley et al.* [2016b]. (b) Nutrient model: note that assimilation of P and N only occurs in the surface water (SW) reservoirs, denitrification, and burial only in the deepwater (DW) reservoirs (gray dashed arrows). Assim = assimilation; sol = solubilization; min = mineralization; nit = nitrification.

released to solution in seawater. Dissolved reactive P encompasses PO_4 and DOP. Likewise reactive N is the sum of NO_3, PON, DON, and NH_4, while dissolved reactive N only includes NO_3, DON, and NH_4. Assuming that particulate inorganic N is negligible, total N (TN) equals reactive N. Dissolved inorganic N (DIN) is the sum of NO_3 and NH_4.

The P and N concentrations in the water reservoirs and the corresponding ranges obtained from the literature are given in Table 1. Note that the concentration values are those obtained after spinning the model up to steady state. The WMS and EMS nutrient models are coupled via the fluxes of the various forms of dissolved P and N through the Strait of Sicily. The following sources of P and N to the WMS are considered: inflow of ASW via the Strait of Gibraltar, atmospheric deposition, river inflow, submarine groundwater discharge (SGD), and direct domestic wastewater discharges. In addition, and in contrast to the EMS, N_2 fixation represents a non-negligible input of reactive N to the WMS [*Garcia et al.*, 2006; *Sandroni et al.*, 2007; *Ibello et al.*, 2010; *Bonnet et al.*, 2011] and is therefore explicitly included. The estimated P and N input fluxes from direct wastewater discharges [*Powley et al.*, 2016a] and SGD [*Rodellas et al.*, 2015] are based on recent studies.

Table 1. Reactive P and N Concentrations After Model Spin-Up and Ranges (in Brackets) From the Literature[a]

	PO_4	POP	DOP	NO_3	PON	DON	NH_4
	nM			μM			
WMS							
SW	48 (0–350)	17 (1–100)	72 (0–400)	0.8 (0–7.3)	0.4 (0.1–2.2)	2.8 (2.0–7.5)	0.03 (0–0.06)
IW	269 (40–470)	8 (0–55)	44 (0–140)	6.6 (1.4–9.9)	0.1 (0.01–0.3)	2.7 (0.1–4.6)	0.01 (0–0.007)
DW	369 (140–480)	3 (0–15)	27 (0–140)	7.7 (1.6–9.5)	0.05 (0.00–0.4)	2.5 (1.4–6.7)	0.01 (nd[b])
EMS							
SW	23 (0–100)	7 (4–20)	47 (10–100)	0.6 (0.01–3)	0.3 (0.1–0.5)	2.7 (2–11)	0.09 (0.04–0.08)
IW	102 (30–200)	5 (3–10)	40 (30–80)	2.6 (0.5–6)	0.2 (0.1–0.3)	2.7 (2–5)	0.05 (0.05–0.06)
DW	169 (130–230)	3 (2.5–8)	38 (0–70)	4.8 (3–6)	0.1 (0.05–0.15)	2.6 (0–5)	0.05 (<0.1)

[a]Literature ranges for the WMS are from Tables S1 and S2 and for the EMS from *Van Cappellen et al.* [2014].
[b]nd = no data.

Because they were not considered in the original EMS model, the latter is updated as described in section 2.3. The outputs of P and N considered in the model are sedimentary burial, outflows to adjacent basins, and for N also denitrification. All references used to initialize model reservoirs, external inputs, and outputs are given in Table 2.

2.3. External Inputs of P and N

The incoming NO_3 flux from the Atlantic Ocean is calculated using reported NO_3 concentrations in the Strait of Gibraltar [*Huertas et al.*, 2012], corrected for the effect of solute mixing within the strait [*Macias et al.*, 2007] (see the supporting information for details). The corresponding PO_4 flux is calculated using a NO_3:PO_4 ratio of 10:1 [*Coste et al.*, 1984; *Gómez et al.*, 2000; *Dafner et al.*, 2003; *Huertas et al.*, 2012]. Concentrations of DON (4.5 μM) and DOP (0.14 μM) in the incoming ASW are derived from data from Station 7, west of the Strait of Gibraltar, measured during the MEDRIPOD IV cruise [*La Corre et al.*, 1984]. Nutrient concentrations are multiplied by the ASW inflow of 0.83 Sv (10^6 m^3 s^{-1}) (for justification, see *Powley et al.* [2016b]) to yield the input fluxes listed in Table 3. In a similar fashion, the inputs of the various P and N species from the EMS are computed by multiplying the EMIW concentrations by the inflow via the Strait of Sicily.

Table 2. Summary of References Used for Initialization of the Steady State Model Reservoirs and Fluxes[a]

	References
P and N reservoir concentrations	[*McGill*, 1961; *Banoub and Williams*, 1972; *Millero et al.*, 1978; *Copin-Montegut and Copin-Montegut*, 1983; *Coste et al.*, 1984; *Béthoux et al.*, 1992; *Pujo-Pay et al.*, 1995; *Béthoux et al.*, 1998; *Doval et al.*, 1999; *Moutin and Raimbault*, 2002; *Lucea et al.*, 2003; *Aminot and Kérouel*, 2004; *Schroeder et al.*, 2010; *Pujo-Pay et al.*, 2011; *Tanhua et al.*, 2013]
Input Fluxes	
Atlantic surface water P and N concentrations	[*Coste et al.*, 1984; *La Corre et al.*, 1984; *Coste et al.*, 1988; *Gómez et al.*, 2000; *Doval et al.*, 2001; *Dafner et al.*, 2003; *Macias et al.*, 2007; *Huertas et al.*, 2012; *Schroeder et al.*, 2012; *Ramirez-Romero et al.*, 2014]
Atmospheric deposition	[*Migon et al.*, 1989; *Loÿe-Pilot et al.*, 1990; *Bergametti et al.*, 1992; *LeBolloch and Guerzoni*, 1995; *Guerzoni et al.*, 1999; *Migon and Sandroni*, 1999; *Migon et al.*, 2001; *Sandroni et al.*, 2007; *Markaki et al.*, 2010; *Nenes et al.*, 2011; *Powley et al.*, 2014; *Van Cappellen et al.*, 2014; *Stockdale et al.*, 2016]
Submarine groundwater discharge	[*Dowling et al.*, 2003; *Burnett et al.*, 2006; *Burnett et al.*, 2007; *Charideh and Rahman*, 2007; *Kroeger et al.*, 2007; *Santos et al.*, 2009; *Garcia-Solsona et al.*, 2010; *Bayari et al.*, 2011; *Erisman et al.*, 2011; *Weinstein et al.*, 2011; *El-Gamal et al.*, 2012; *Asai et al.*, 2013; *Kim et al.*, 2013; *Santos et al.*, 2013; *Makings et al.*, 2014; *Tait et al.*, 2014; *Tovar-Sanchez et al.*, 2014; *FAOSTAT*, 2015b, 2015a, *Rodellas et al.*, 2015]
Rivers	[*Ludwig et al.*, 2009; *Van Cappellen et al.*, 2014]
Domestic wastewater	[*Powley et al.*, 2016a]
N_2 fixation	[*Garcia et al.*, 2006; *Sandroni et al.*, 2007; *Ibello et al.*, 2010; *Bonnet et al.*, 2011]
Output Fluxes	
Burial of P and N	[*Aspila et al.*, 1976; *Sanchez-Cabeza et al.*, 1999; *Van Den Broeck and Moutin*, 2002; *de Madron et al.*, 2003; *Denis and Grenz*, 2003; *Masqué et al.*, 2003; *Zúñiga et al.*, 2007a; *Zúñiga et al.*, 2007b; *Ruttenberg et al.*, 2009; *Heimbürger et al.*, 2012]
Denitrification	[*Gehlen et al.*, 1997; *Denis and Grenz*, 2003]

[a]See section 2 of main text and supporting information for more details.

Table 3. Input and Output Fluxes of P (PO_4, POP, and DOP) and N (NO_3, DON, NH_4, and PON) for the WMS and EMS (in Units of 10^9 mol yr^{-1})

	Sea	PO_4	DOP	POP	NO_3	DON	NH_4	PON
Input								
Riverine	WMS	0.14	0.01		2.9	0.8	0.2	
	EMS	0.23	0.06		2.4	0.6	0.2	
Atmospheric	WMS	0.16	0.15		8.1	12.3	5.8	
	EMS	0.38	0.33		19.8	30.8	13.8	
N_2 fixation	WMS							12.1
	EMS							0
SGD[a]	WMS	0.008	0.004		1.1	3.3	0.01	
	EMS	0.004	0.002		0.4	1.8	0.01	
Wastewater	WMS	0.17	0.03	0.08	0.7	0.4	2.1	0.2
	EMS	0.13	0.02	0.05	0.2	0.4	2.0	0.2
Output								
Burial	WMS			0.55				10.6
	EMS			0.71				20.7
Denitrification	WMS				18.0			
	EMS				2.4			
Inflow/Outflow From Adjacent Basins								
Atl − WMSW (Concentration)[b]		4.05 (0.155)	3.66 (0.14)		41.8 (1.6)	117.5 (4.5)	2.6 (0.1)	
WMSW − EMSW		1.72	2.60		29.4	100.0	1.1	
EMIW − WMIW		3.52	1.39		90.5	93.2	1.6	
WMIW − Atl		3.97	0.65		97.3	40.4	0.1	
WMDW − Atl		3.63	0.27		76.2	24.4	0.1	
EMIW − Adr		1.02	0.40		26.3	27.1	0.5	
Adr − EMDW		1.08	0.42		28.5	29.9	0.5	
EMIW − Aeg		0.13	0.05		3.3	3.4	0.1	
Aeg − EMDW		0.14	0.05		3.7	3.6	0.1	
(WMSW + WMIW) − NWM		3.57	1.05		84.9	53.0	0.3	
NWM − WMDW		3.57	1.05		85.2	53.1	0.3	

[a]SGD = freshwater-derived submarine groundwater discharge.
[b]μM.

The 1950 riverine inputs of TP and TN to the WMS are assigned the values estimated by *Ludwig et al.* [2009] for 1963, assuming that minimal change occurred between 1950 and 1963. Riverine TP is assumed to consist of 48% PO_4, 8% DOP, and 44% PIP, while riverine TN is 75% NO_3, 20% DON, and 5% NH_4 [*Ludwig et al.*, 2009] It is further assumed that 75% of PIP solubilizes to PO_4 upon addition to seawater [*Van Cappellen et al.*, 2014]. The 1950 riverine fluxes of dissolved reactive P and dissolved reactive N to the WMS are then equal to 0.16×10^9 mol P yr^{-1} and $3.9 \times$ mol N yr^{-1} (Table 3).

Atmospheric deposition in the WMS has two main sources: Saharan dust and anthropogenic emissions from Europe, mainly from industry and transportation [*Bergametti et al.*, 1992]. The estimated average total deposition fluxes of leachable inorganic P and inorganic N measured over the period of 1984–2005 are 0.37×10^9 mol P yr^{-1} and 36.7×10^9 mol N yr^{-1}, respectively (section S1.1.2 and Table S3 in the supporting information). We further estimate that 38% of leachable P and 32% of leachable N in atmospheric deposition are in the form of DOP and DON, respectively [*Markaki et al.*, 2010; *Van Cappellen et al.*, 2014]. The resulting atmospheric fluxes of reactive P and N are representative of the 1990s and are therefore back-projected to 1950 values using the forcing functions presented in *Powley et al.* [2014]. These functions are derived from (1) ice core records for NO_3 and NH_4 deposition, (2) sulfur and NO_x emissions for PO_4 deposition as they cause acid processing of atmospheric dust thereby increasing P solubility [*Nenes et al.*, 2011; *Stockdale et al.*, 2016], and (3) biomass burning trends to account for changes in atmospheric deposition of DOP and DON. The resulting 1950 values, imposed in the model, are listed in Table 3.

Nitrogen fixation has been suggested to account for 38–53% of the total external N input to the MS (or 50–90×10^9 mol N yr^{-1}) in order to balance the N budget [*Béthoux et al.*, 1992]. However, direct measurements of N_2 fixation within the MS have only recently been undertaken, yielding estimates between 0.97×10^9 and

29×10^9 mol N yr^{-1} for the whole WMS [*Garcia et al.*, 2006; *Sandroni et al.*, 2007; *Ibello et al.*, 2010; *Bonnet et al.*, 2011]. Here, N_2 fixation is assigned a flux of 12.1×10^9 mol N yr^{-1} based on data obtained during the BOUM cruise along an east to west transect across the WMS [*Bonnet et al.*, 2011].

Recent estimates of the direct domestic wastewater discharges of TP and TN into the WMS in year 2003 are 0.35×10^9 mol P yr^{-1} and 5.4×10^9 mol N yr^{-1} [*Powley et al.*, 2016a]. Wastewater TP is assumed to comprise 43% PO_4, 25% POP, 10% DOP, and 22% PIP, while wastewater TN consists of 16% NO_3, 7% PON, 12% DON, and 65% NH_4 [*Powley et al.*, 2016a]. The 1950 reactive N input fluxes are obtained from the corresponding 2003 values by assuming that direct domestic wastewater N discharges scale proportionally to the coastal population [*FAOSTAT*, 2016]. For reactive P, direct domestic wastewater is assumed to follow riverine N:P trends, hence accounting for changes in laundry and dishwasher detergent use between 1950 and 2003.[*Ludwig et al.*, 2009, 2010]. The resulting 1950 input fluxes are given in Table 3.

Submarine groundwater discharges of PO_4 and DIN are calculated by multiplying the flow of fresh SGD into the WMS [*Powley et al.*, 2016b] and the average PO_4 and DIN concentrations in Mediterranean coastal aquifers [*Rodellas et al.*, 2015]. Imposing a NO_3:DIN ratio of 0.99 (Table S4), and assuming that DOP and DON contribute one third of dissolved reactive P and N in SGD, respectively (Table S5), yields SGD fluxes of 0.015×10^9 mol P yr^{-1} and 14.4×10^9 mol N yr^{-1} for the early 2000s. The 1950 reactive N flux from SGD (Table 3) is then derived from fertilizer and manure application trends [*Erisman et al.*, 2011; *FAOSTAT*, 2015a, 2015b] and assuming a 30 year time lag between SGD recharge and discharge (Table S6). We further assume that anthropogenic inputs of reactive P are retained in the aquifers due to the low dissolved reactive P concentration in SGD reported for the early 2000s [*Rodellas et al.*, 2015]. Thus, the 1950 dissolved reactive P flux from 1950 is the same as that for the early 2000s.

2.4. Outputs of P and N

Fluxes of dissolved reactive P and N exiting the WMS through the Strait of Gibraltar are calculated by multiplying the corresponding water fluxes with the concentrations of the various P and N species in WMIW and WMDW (Tables 1 and 3). Similarly, the outputs of dissolved reactive P and N to the EMS are obtained by multiplying the concentrations in WMSW with the flow of water from the WMS to the EMS via the Strait of Sicily.

To the authors' knowledge, no published estimates exist for POP burial in the WMS. We therefore obtained samples from eight sediment cores from the Alboran Sea and Catalan Shelf, courtesy of Dr. Pere Masqué (T6, Alb 1, Alb 2, Alb E, Alb D, T3, EB2, and CN36 [*Sanchez-Cabeza et al.*, 1999; *Masqué et al.*, 2003]) and measured POP concentrations following the SEDEX protocol [*Ruttenberg et al.*, 2009]. Briefly, TP was determined by ashing the sample for 2 h at 500°C, followed by 16 h of 1 M HCl digestion; PIP was measured after 16 h of 1 M HCl digestion. The POP concentration was calculated as the difference between the two experimental values (see the supporting information for details on the core locations and experimental methods and results).

The POP concentration of sediment samples varies by only a factor of 2 (2.9–7.1 μmol g^{-1} dry weight; Table S9), in contrast to reported sediment accumulation rates which vary by an order of magnitude (0.063–0.51 g cm^2 yr^{-1}; Table S8 [*Sanchez-Cabeza et al.*, 1999; *Masqué et al.*, 2003]). The open WMS POP burial flux is estimated using the average POP sediment concentration measured in the cores retrieved at water depths exceeding 1000 m (5.6 μmol g^{-1} dry weight), multiplied by sediment accumulation rates from the Algero-Balearic basin (41 g m^{-2} yr^{-1} [*Zúñiga et al.*, 2007a]) and DYFAMED site (168 g m^{-2} yr^{-1} [*Heimbürger et al.*, 2012]) (Table S7). Burial of POP in the Alboran Sea is estimated using the average POP burial rate from the six cores located in the Alboran Sea. The sediment POP concentrations for the Catalan shelf (core CN 36) together with reported sediment accumulation rates are used to approximate POP burial in the Gulf of Lions [*Van Den Broeck and Moutin*, 2002] (Table S10). The resulting range for the POP burial flux in the WMS is then $0.56–1.1 \times 10^9$ mol P yr^{-1} (Table S7). We use the low-end estimate as representative of the 1950 POP burial flux. The final burial flux after model spin-up is reported in Table 3.

Sediment PON burial is estimated separately for the Alboran Sea, Gulf of Lions, and the remaining WMS, using reported burial rates of PON [*Masqué et al.*, 2003; *Heimbürger et al.*, 2012] and POC [*de Madron et al.*, 2003;

Zúñiga et al., 2007a]. To convert from POC to PON burial rates, molar POC:PON ratios of 9.4 and 5.5 are assigned to the Gulf of Lions [*Denis and Grenz*, 2003] and the open WMS [*Zúñiga et al.*, 2007b], respectively. The resulting total PON burial flux for the WMS is on the order of 11×10^9 mol yr^{-1} (see Table S7). The denitrification flux for the WMS (20×10^9 mol yr^{-1}; see Table S11) is derived from denitrification rates measured over the course of 1 year at the DYFAMED site [*Gehlen et al.*, 1997], plus sediment core incubation results for the Gulf of Lions [*Denis and Grenz*, 2003]. Slight adjustments after model spin-up yield the N removal fluxes given in Table 3.

2.5. Primary Production

Annual primary productivity in the WMS is assigned to be 2.5 times that in the EMS based on the primary production measurements in the WMS and EMS between 1970 and 2010 compiled by *Berman-Frank and Rahav* [2012]. The resulting 1950 primary productivity in the WMS after model spin-up is then 148 g C m^{-2} yr^{-1}, compared to 56 g C m^{-2} yr^{-1} in the EMS. Primary productivity is converted to P and N assimilation fluxes using the Redfield C:N:P ratio of 106:16:1 [*Redfield et al.*, 1963]. At steady state, export production equals new production [*Eppley and Peterson*, 1979]. The export production in the WMS is 28–35 g C m^{-2} yr^{-1} according to *Béthoux* [1989] and *Zúñiga et al.* [2008]. Using molar POC:PON and POC:POP ratios of sinking organic matter of 7.7 and 169, respectively [*Marty et al.*, 2009], we obtain export fluxes of 11.4–14.1 $\times 10^9$ mol yr^{-1} for POP and 259–318 $\times 10^9$ mol yr^{-1} for PON. The lower values of these two ranges are assigned to the 1950 fluxes of POP and PON from WMSW to WMIW, in order to account for the increased productivity since 1950, because of higher inputs of anthropogenic nutrients to the MS [*Ludwig et al.*, 2009; *Powley et al.*, 2014, 2016a]. The final sinking fluxes upon model spin-up are given in Table S12.

2.6. Deepwater Formation

Incoming WMDW through DW formation in the NWM contains the dissolved reactive P and N originally present in the WMSW and WMIW exported to the NWM. A small correction for additional external inputs to the NWM from N_2 fixation and atmospheric deposition is applied to the deepwater P and N fluxes into the WMDW similar to the approach used by *Van Cappellen et al.* [2014] for the EMS. Total reactive dissolved fluxes of 4.6×10^9 mol P yr^{-1} and 139×10^9 mol N yr^{-1} are then estimated to enter the WMDW through DW formation in 1950, of which 0.009 × mol P yr^{-1} and 0.43×10^9 mol N yr^{-1} are attributed to the additional external inputs into the NWM (Table 3; see the supporting information for further details).

2.7. Modifications to Existing EMS Model

The original EMS model of *Van Cappellen et al.* [2014] is modified by adding SGD and direct domestic wastewater discharges as sources of P and N, following the same procedures as for the WMS (section 2.3). The EMS wastewater reactive P and N inputs for the year 2003 of *Powley et al.* [2016a] are reduced taking into account the changes in the coastal populations and riverine N:P ratios [*Ludwig et al.*, 2009; *FAOSTAT*, 2016], to yield 1950 wastewater fluxes into the EMS of 0.2×10^9 and 2.7×10^9 mol yr^{-1} for reactive P and N, respectively. The 1950 dissolved reactive P and N fluxes associated with SGD are computed using a fresh SGD water flux to the EMS of 15.1 km^3 yr^{-1} derived from regional estimates by *Zekster et al.* [2007], PO_4 and DIN concentrations of 0.28 and 370 μM, respectively [*Rodellas et al.*, 2015], and assuming that DOP and DON contribute one third of the reactive P and N inputs (section 2.3). The additional P and N inputs cause slight changes to the EMS model; the largest ones involve adjustments of the first-order rate constants (k) for P solubilization and mineralization in EMDW, N mineralization in EMIW and EMDW, and EMDW nitrification. These changes, however, are within 9% of the original k values. All other k values remain unchanged.

2.8. Numerical Solution and Sensitivity Analyses

The model consists of 42 differential equations that are solved simultaneously in MATLAB with solver ODE15s. The numerical approach followed is the same as described by *Van Cappellen et al.* [2014] for the EMS model. The fluxes in the model are described by simple first-order rate expressions with respect to the source reservoir mass. Exceptions are the turbulent diffusion fluxes, which depend linearly on the concentration differences between source and sink reservoir. Vertical eddy diffusion coefficients are the same as in *Powley et al.* [2016b]. Slightly modified rate expressions are also used to represent DON mineralization and nitrification in the WMSW and EMSW [see *Van Cappellen et al.*, 2014]. Upwelling and downwelling fluxes,

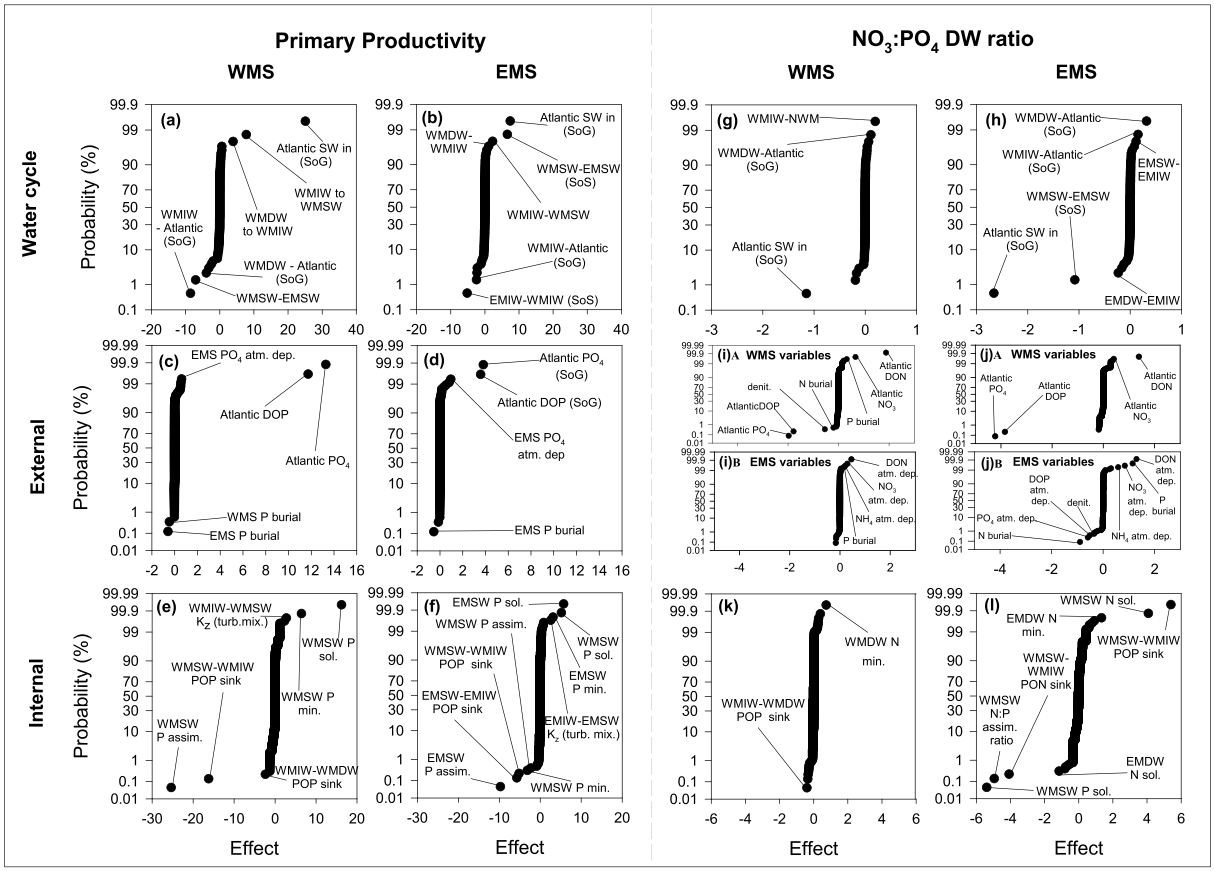

Figure 2. Factorial design analysis: panels show the sensitivity of two model outcomes, (a–f) primary productivity and (g–l) the DW NO_3:PO_4 ratio, in the WMS and EMS to various sets of model variables associated with the MS water cycle (Figures 2a, 2b, 2g, and 2h), external P and N sources (Figures 2c, 2d, 2i, and 2j), and processes occurring within the MS (Figures 2e, 2f, 2k, and 2l). See text for details. SoG = Strait of Gibraltar; SoS = Strait of Sicily; atm.dep. = atmospheric deposition; denit. = denitrification; assim. = assimilation; sol. = solubilization; min = mineralization; turb. mix = turbulent mixing.

along with the bidirectional fluxes between the EMS and WMS through the Strait of Sicily, are computed from the nutrient concentrations in the source reservoir and the corresponding water flow to the receiving water body [*Powley et al.*, 2016b]. Final model values for the internal nutrient fluxes (Table S12) and corresponding rate parameters (k) are obtained by spinning the model up to steady state.

A global model sensitivity analysis is carried out with a fractional factorial design analysis [*Box et al.*, 1978; *Van Cappellen et al.*, 2014] of the coupled WMS-EMS model. Four model responses are tested (WMS and EMS primary productivity, and WMS and EMS NO_3:PO_4 DW ratio) using three sets of parameters: water cycle (2^{14-4} fractional factorial design), internal fluxes (2^{46-36} fractional factorial design), and external fluxes. For the latter, a 2^{28-18} factorial design analysis is used to assess the sensitivity of primary productivity, while due to the high number of variables, the responses of NO_3:PO_4 DWratios are investigated separately for the WMS and EMS variables. Model parameters within each set are varied by ±10%. Thus, for example, when internal parameters are varied, external and water cycle parameters remain constant. Results are plotted on effect versus probability graphs. Because higher-order effects have negligible effects on the model dynamics [*Van Cappellen et al.*, 2014], only first- and second-order interactions are plotted. Results that deviate from the vertical axis through the origin imply that the model response is sensitive to the corresponding parameter.

The sensitivity analyses indicate that primary productivity in both the WMS and EMS is particularly sensitive to inflow of PO_4 and DOP from the Atlantic Ocean, plus atmospheric deposition of PO_4 in the respective basins (Figures 2a–2d). Primary productivity in both WMS and EMS is also sensitive to the solubilization of POP and subsequent mineralization of DOP within the SW, highlighting the role of heterotrophic

processes in recycling P, as well as to other internal cycling processes such as P assimilation, sinking of POP out of the SW, and, in the EMS, turbulent mixing (Figures 2e and 2f). Interestingly, primary productivity in the EMS is sensitive to processes in the WMSW that are involved in the recycling of P and the fluxes of P into and out of WMSW (Figure 2f).

The WMDW NO_3:PO_4 ratio is most sensitive to the inflow of PO_4 and DON from the Atlantic Ocean, together with atmospheric DON deposition in the EMS (Figures 2g, 2i, and 2k). For EMDW, the NO_3:PO_4 ratio is more sensitive to processes that alter the N:P of the water entering the DW rather than processes taking place in the EMDW reservoir itself (Figures 2h, 2j, and 2l). Furthermore, the EMDW NO_3:PO_4 ratio is more sensitive to processes taking place in the WMS, such as sinking of POP out of WMSW, N:P assimilation ratio in the WMSW, solubilization of POP and PON in the WMSW, and dissolved P and N entering the WMS through the Strait of Gibraltar, than to any process occurring in the EMS. For example, increasing the WMSW solubilization flux of PON by 10% results in a 7% increase in the EMDW NO_3:PO_4 ratio (Table S14). In comparison, a 10% change in the EMSW or EMDW PON solubilization flux only changes the EMDW NO_3:PO_4 ratio by 0.1 and 1.5%, respectively. Overall, the sensitivity analyses also suggest that the EMDW NO_3:PO_4 ratio is more prone to change than the WMDW NO_3:PO_4 ratio.

When the model is run with a NO_3:PO_4 uptake ratio of 23:1 during SW assimilation (see section 2.2), it is possible to reproduce the same water column distributions of P and N concentrations in the WMS and EMS than with the 16:1 uptake ratio, if the rate constants (k) describing the recycling of PON in the SW (i.e., solubilization, ammonification, and nitrification) are increased by about 40%. In other words, variations in the photosynthetic NO_3:PO_4 uptake ratio can be compensated by adjusting the recycling efficiency of PON in the SW reservoirs accordingly. However, the trends in DW NO_3:PO_4 ratios and the conclusions regarding the recycling of P and N within the two basins remain unchanged and are thus robust model results.

3. Results and Discussion

The coupled WMS-EMS model represents the external sources, biogeochemical transformations, physical redistribution within and between the two basins, and ultimate sinks of the two nutrient elements P and N. Here we analyze the features of the modeled P and N cycles before the large increases in anthropogenic nutrient inputs that took place during the second half of the twentieth century. The steady state P and N model fluxes in 1950 thus provide the quantitative basis for interpreting some of the characteristic and unusual biogeochemical properties of the MS prior to their large-scale perturbation by human activity. The changes in the P and N cycles that occurred since 1950 are the topic of a companion study. It is important to recognize the limitations of the model. In particular, the simple physical and biogeochemical structure of the model does not account for lateral variations in nutrient distributions and process rates in the WMS and EMS, nor does it resolve sub-annual features of the P and N cycles. Instead, the model aims to reproduce the basin-wide, yearly averaged fluxes and transformations of the nutrients elements.

3.1. External Phosphorus and Nitrogen Inputs to the MS

Because it is nearly entirely surrounded by land, one might expect terrestrial sources to dominate the inputs of reactive P and N to the MS. However, according to our estimations, the main source of P and N to the MS is inflow of ASW through the Strait of Gibraltar, which provides 79% of reactive P and 56% of reactive N inputs to the entire MS (Figure 3 and Table 3). The aggregated supplies of non-marine reactive P and N, that is, the combined inputs from atmospheric deposition, rivers, SGD, direct wastewater discharges, N_2 fixation, and additional reactive P and N from the NWM and the Adriatic and Aegean Seas, are similar for the WMS and EMS when normalized per unit surface area: approximately 0.001 mol P m^{-2} yr^{-1} and 0.06 mol N m^{-2} yr^{-1}. By contrast, the inputs of marine sourced reactive P and N are 4 to 5 times greater for the WMS than the EMS. The combined inputs of ASW and EMIW entering the WMS through the Straits of Gibraltar and Sicily amount to 0.015 mol P m^{-2} yr^{-1} and 0.4 mol N m^{-2} yr^{-1}, while only 0.003 mol P m^{-2} yr^{-1} and 0.1 mol N m^{-2} yr^{-1} enter the EMS with inflow of WMSW through the Strait of Sicily (Figure 3).

The estimated external nutrient inputs therefore reveal a key difference between the WMS and EMS. For the WMS, non-marine reactive P and N fluxes are added to a relatively enriched background of reactive P and N that originate from the North Atlantic and EMIW. In contrast, for the EMS, the comparable non-marine reactive P and reactive N inputs are added to inflow of WMSW through the Strait of Sicily that is severely depleted

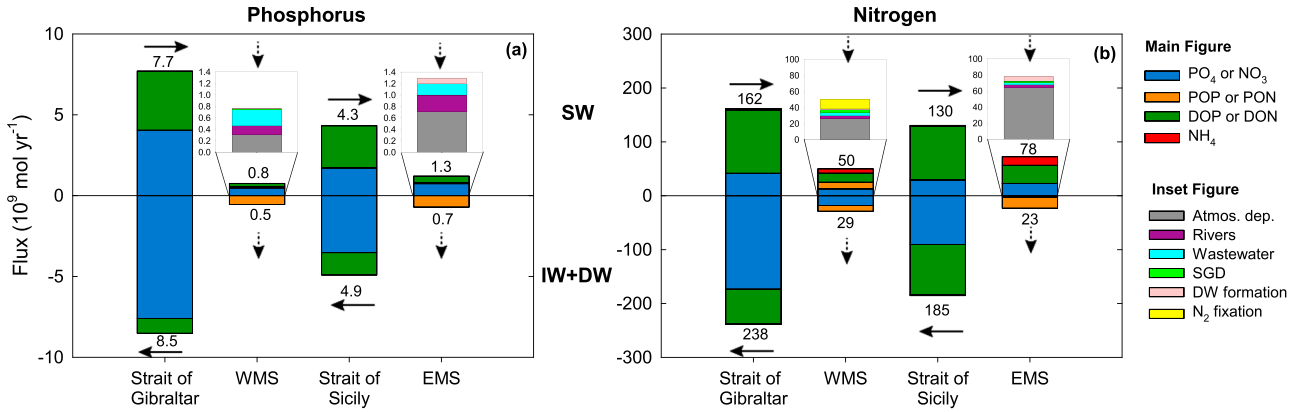

Figure 3. Speciation of (a) phosphorus and (b) nitrogen in the inputs to and outputs from the MS in the year 1950. The numbers at top and bottom of the columns represent total fluxes in 10^9 mol yr^{-1}. The horizontal arrows indicate direction of flow of water through the Strait of Gibraltar and the Strait of Sicily; the vertical arrows indicate input (positive numbers) and output (negative numbers) of P and N for the WMS and EMS (excluding the exchanges through the straits). The removal of POP or PON in the WMS and EMS is due to burial in sediments; the removal of NO_3 corresponds to denitrification. The inset figures represent the contributions of different external inputs to the WMS and EMS (excluding flows through the straits). See Table 3 for numerical values. DW formation = the additional P and N acquired during deepwater formation in the north-west Mediterranean (NWM) for the WMS and Adriatic and Aegean Seas for the EMS.

in reactive P and reactive N as observed by *Ribera d'Alcala et al.* [2009], *Karafistan et al.* [2002], and *Denis-Karafistan et al.* [1998].

3.2. Primary Production and New Production

The significantly higher marine-derived reactive P input to the WMS, compared to the EMS, largely explains the difference in primary productivity between the two basins. (Note that here we focus on reactive P inputs, as the model assumes that the yearly averaged primary productivities of the WMS and EMS are P limited.) The total reactive P input flux to the WMS is 3.9 times greater per m^2 than for the EMS (Table 3), while primary production is 2.6 times greater in the WMS (148 versus 56 g C m^{-2} yr^{-1} in the WMS and EMS, respectively). If only external inputs to SW are considered (i.e., excluding internal inputs associated with upwelling and turbulent mixing), WMSW receives 2.5 times more reactive P per m^2 than EMSW (0.01 versus 0.004 mol P m^{-2} yr^{-1}).

In addition to the large difference in external reactive P inputs, the two basins diverge in their thermohaline circulation (Figure 1). In the WMS upwelling (from WMIW to WMSW) brings additional dissolved reactive P (and N) into the photic zone. In contrast, the thermohaline circulation of the EMS is dominated by downwelling (from EMSW to EMIW), which removes dissolved nutrients from the surface waters. The dissolved reactive P (and N) accumulating in EMIW is largely exported through the Strait of Sicily to the WMS. In the EMS, turbulent mixing is the only internal transport process providing additional reactive P to the photic zone. As a result, the WMS and EMS not only differ in their primary production but also in their new production.

Here, new production is defined as the portion of yearly primary production that is supported by sources of dissolved reactive P supplied from outside the SW reservoir. We assume that all recycled production from the solubilization of POP in SW is regenerated and that the difference between DOP mineralization and POP solubilization is the new production supported by DOP (see Figure 1 for model schematic). Overall, 39% of new production in the WMS is sustained by dissolved reactive P delivered with the inflow of ASW and 45% by upwelling of WMIW (Figure 4). In comparison, in the EMS 37% of new production is supported by inflow of WMSW and 48% by turbulent mixing (Figure 4). Thus, in both basins large fractions of new production are due to the lateral transfer of (marine) nutrients via surface flow through the Straits of Gibraltar and Sicily. The new production estimates further suggest that 26% and 37% of DOP supplied to WMSW and EMSW, respectively, are remineralized and potentially used for autotrophic assimilation. This is a significant finding, given that the dissolved organic pools of P and N are usually not considered to be important sources of new production in marine systems.

The MS is therefore unusual not only because of the important role lateral flows play in supplying P (and N) to the photic zone but also because of the large fractions of new production that are supported by DOP (and

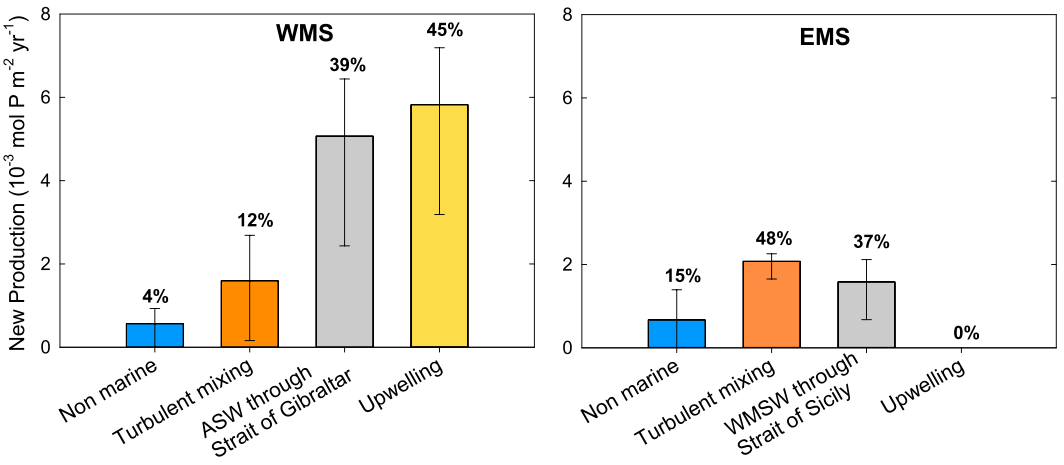

Figure 4. Source attribution of new production in the WMS and EMS. The percentages represent the relative contribution of each source; the error bars represent the uncertainty of individual source contributions for a total new production of 10.6×10^9 mol P yr^{-1} in the WMS and 5.8×10^9 mol P yr^{-1} in the EMS.

DON). *Van Cappellen et al.* [2014] previously proposed that DOP constitutes a major fraction (about 60%) of reactive P entering the EMS from the WMS and that it contributes a substantial portion of new production in the EMS. Similarly, inflow of ASW through the Strait of Gibraltar comprises a large fraction (47%) of reactive P in the form of DOP (Figure 3a and Table 3). However, not all DOP entering the WMSW and EMSW is used for new production but instead gets removed by downwelling and lateral outflow. In fact, our calculations imply that 74 and 63% of DOP entering the WMSW and EMSW, respectively, leave the SW reservoirs without contributing to export production. It is likely that the DOP thus removed from the SW is mainly refractory, given that both the WMS and especially the EMS exhibit high levels of alkaline phosphatase activity [*Zaccone et al.*, 2012] (see also section 3.4).

The importance of the lateral supply of nutrients to the SW of the MS, particularly as DOP and DON, bears a strong resemblance to the recent hypothesis developed by *Letscher et al.* [2016] for subtropical gyres. These authors propose that lateral advection is a major source of nutrients supporting new production in subtropical oceanic gyres, in addition to vertical mixing. They estimate that lateral supplies of P and N support 44–67% and 24–36% of new production in subtropical gyres, respectively, with the lateral supply of DOP and DON contributing 22–46% and 12–19% of export production, respectively. That the MS behaves similarly to open ocean gyres with respect to lateral nutrient supply may at first seem surprising given that it is an almost entirely landlocked marine basin. The reason stems from the anti-estuarine circulation, which drives the large lateral inflow of ASW, and its associated nutrient load, into the MS.

The model-derived new production equals 10.6×10^9 mol P yr^{-1} in the WMS and 5.8×10^9 mol P yr^{-1} in the EMS. In comparison, total primary production, expressed as P assimilation in the SW, equals 95×10^9 mol P yr^{-1} in the WMS and 59×10^9 mol yr^{-1} in the EMS. Thus, recycled production through organic matter breakdown by far exceeds new production in both WMSW and EMSW, accounting for 89–90% of primary production. The resulting *f* ratio, that is, the ratio of new production to primary production [*Eppley and Peterson*, 1979], is slightly lower in the EMS (0.10) than WMS (0.11). The low *f* ratios for both WMS and EMS are typical of oligotrophic marine water bodies; they are similar to other values reported for the MS [*Béthoux*, 1989; *Béthoux et al.*, 1998; *Diaz and Raimbault*, 2000; *Kouvarakis et al.*, 2001; *L'Helguen et al.*, 2002], the Sargasso Sea [*Mongin et al.*, 2003] and the equatorial Pacific [*McCarthy et al.*, 1996].

3.3. Why Is the MS Oligotrophic?

The dominance of ASW as a source of reactive P and N to the MS may seem at odds with the commonly held view that the oligotrophy of the MS is due to the anti-estuarine circulation, which brings in nutrient-depleted surface water into the WMS (EMS) through the Strait of Gibraltar (Strait of Sicily) and returns nutrient enriched water from deeper reservoirs. This view, however, only accounts for the inorganic forms of dissolved P and N. In fact, according to our estimates, the dissolved reactive P flux associated with outflow of WMIW and WMDW

Table 4. Key Model Outputs: Recycling Efficiencies, Residence Times, Inorganic Fractions of Total P and N Inputs, and Integrated Inorganic P and N Contents Across the Entire Water Column[a]

	POM Recycling Efficiency (%)			Residence Time (Years)			% Inorganic Portion of Inputs		% Inorganic
	SW	IW	DW	SW	IW	DW	Total	To SW	In Water Column
Phosphorus									
WMS	89	65	85	1.4	5.1	40	60	54	88
EMS	90	77	48	2.5	5.4	117	45	45	76
Nitrogen									
WMS	82	68	88	1.5	5.3	38	40	37	71
EMS	83	74	50	3.7	6.0	119	34	34	59

[a]POM = POP or PON.

through the Strait of Gibraltar is only 10% larger than the dissolved reactive P flux entering the WMS with ASW (Figures 3a and Table 3). The key difference, however, is the chemical speciation of the dissolved P: 47% of the ASW P inflow is under the form of DOP compared to only 11% in the outflow (Figure 3a and Table 3). Thus, 88% more PO_4 exits the MS through the Strait of Gibraltar than enters at the surface. A similar speciation switch happens at the Strait of Sicily. While the dissolved reactive P flux leaving the EMS is only 14% greater than the dissolved reactive P flux entering the EMS, PO_4 represents 72% of the EMIW outflow compared to 40% in the WMSW inflow (Figure 3a and Table 3). In other words, for both the WMS and EMS the anti-estuarine circulation exports more readily bioavailable P (i.e., PO_4) than it imports.

In comparison, significantly more dissolved reactive N leaves the MS through the Strait of Gibraltar than enters from the Atlantic (Figure 3b and Table 3), reflecting a higher influence of land-derived inputs for reactive N than for P. The flux of dissolved reactive N leaving the MS through the Strait of Gibraltar is 47% larger than the flux entering as ASW and contains more than 4 times greater NO_3 mass. Similarly, at the Strait of Sicily 42% more N exits the EMS as IW than enters as SW, with 3 times more NO_3 leaving the EMS than flowing in.

3.4. The MS As A Net Heterotrophic System

Heterotrophy of the MS is a consequence of the anti-estuarine circulation combined with the recycling of organic matter supplied externally from marine and non-marine sources. Fluxes of dissolved and particulate organic P and N entering the MS exceed those leaving the MS by outflow through the Strait of Gibraltar and sediment burial: 4.4×10^9 mol organic P yr^{-1} and 183×10^9 mol organic N yr^{-1} enter the MS from marine and non-marine sources in comparison to 2.2×10^9 mol organic P yr^{-1} and 96×10^9 mol organic N yr^{-1} leaving the MS. Based on the differences between DOP and DON inputs and outputs, net heterotrophy in the WMS (0.002 mol P m^{-2} yr^{-1} and 0.08 mol N m^{-2} yr^{-1}) exceeds that of the EMS (0.001 mol P m^{-2} yr^{-1} and 0.03 mol m^{-2} N yr^{-1}). Net heterotrophy of the MS inferred from the model fluxes agrees with the suggestion of *Luna et al.* [2012] that the deeper waters of the MS act as "bioreactors" converting organic P and N into dissolved inorganic nutrients, hence explaining why bacterial enzymatic activities are up to an order of magnitude greater in the MS than in the global ocean.

Duarte et al. [2013] speculate that the excess organic matter supplied to the MS to fuel heterotrophy originates from terrestrial sources, primarily delivered via rivers. Our analysis, however, suggests that most of the DOP and DON supplied to the WMS and EMS is from inflow through the Straits of Gibraltar and Sicily, with atmospheric deposition representing a secondary source (Table 3). In comparison, riverine inputs of DOP and DON are fairly minor.

The concentrations of DOP and DON of IW and DW are similar for the WMS and EMS, or even higher in the EMS, despite the larger reactive P and N inputs and higher PO_4 and NO_3 concentrations of the WMS [*Moutin and Raimbault*, 2002; *Pujo-Pay et al.*, 2011]. Integrated across the entire water column PO_4 and NO_3 account for 76% and 59% of dissolved reactive P and N in the EMS, respectively [*Van Cappellen et al.*, 2014], compared to 88% and 71% in the WMS (Table 4). The differences in nutrient distributions between the two basins can be explained by a faster recycling of DOP and DON to PO_4 and NO_3 in the DW of the

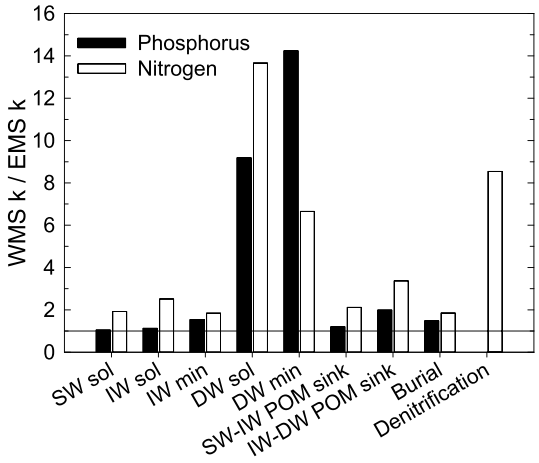

Figure 5. Comparison of first-order rate constants (*k* values in the model) in WMS and EMS. For any given process, a value greater than 1 correspond to a *k* value in the WMS exceeding that in the EMS, and vice versa. The black bars represent *k* values for P fluxes; the white bars represent *k* values for N fluxes. See Figure 1 for the definitions of the processes. POM = POP or PON.

WMS compared to the EMS, with the higher reactive P and N inputs into the WMS supporting greater bacterial activity in the WMS than the EMS [*Luna et al.*, 2012]. In the model, the first-order rate coefficients (*k*) describing DW P solubilization and mineralization are 9 and 14 times greater in the WMS than EMS, respectively (Figure 5).

The model *k* values further suggest that the particulate and dissolved organic P and N in the EMS are less labile than their counterparts in the WMS, especially in the DW reservoirs. This is consistent with the higher cell specific alkaline phosphatase activities measured in EMDW compared to WMDW [*Zaccone et al.*, 2012], which imply greater efforts by the EMS microbial community to access the less available POP and DOP. The longer residence time of EMDW (Figure 1) likely results in the accumulation of refractory organic matter within the EMDW. In contrast, Bernoulli suction forces WMDW out into the Atlantic Ocean through the Strait of Gibraltar, hence actively

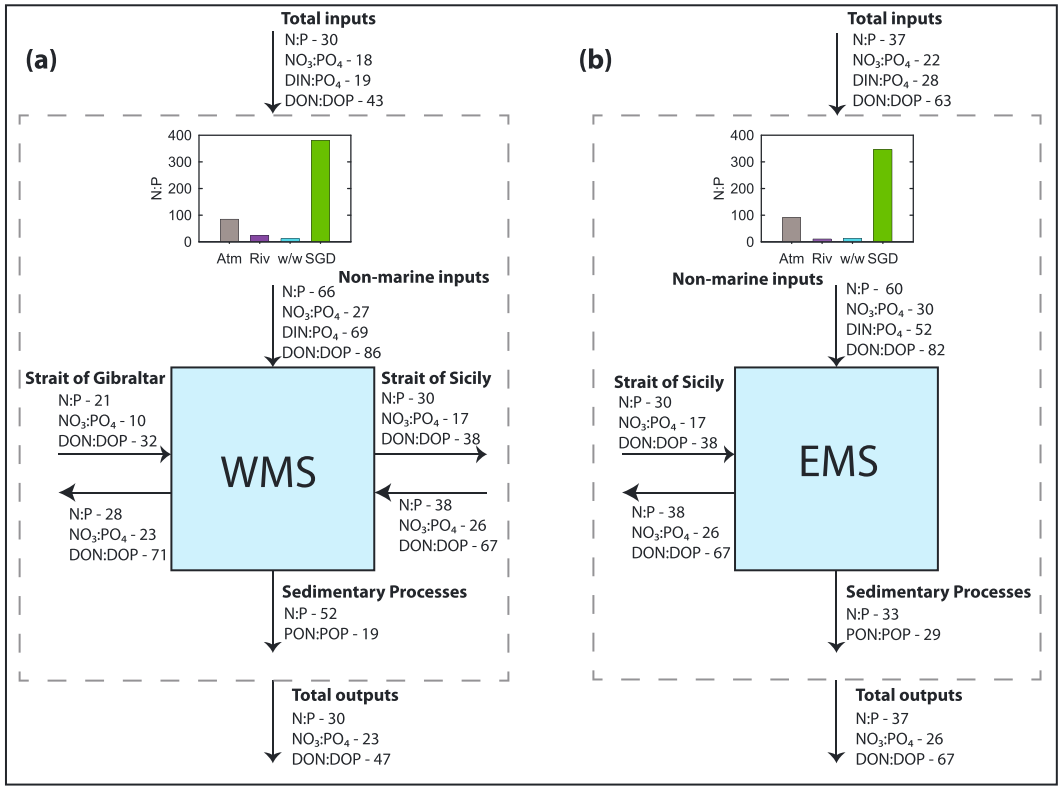

Figure 6. Reactive N:P ratios of input and output fluxes to (a) the WMS and (b) the EMS. $DIN:PO_4$ ratio of fluxes is within 1 unit of $NO_3:PO_4$ ratios unless otherwise stated. The inset figures show the reactive N:P ratios of non-marine sources to the MS. Atm = atmospheric deposition; Riv = riverine input; w/w = direct domestic wastewater discharges; SGD = submarine groundwater discharge.

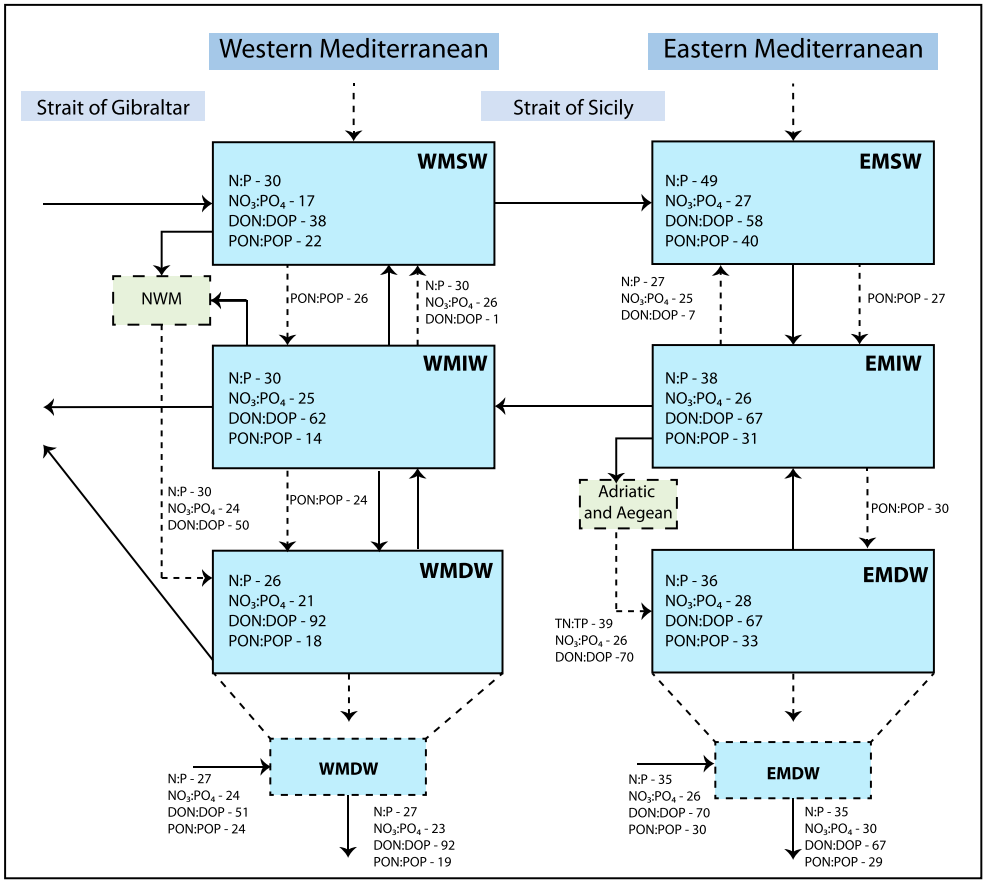

Figure 7. N:P ratios of reservoirs and internal fluxes in the model. The solid arrows represent water flows, and the associated N:P ratios are those of the corresponding source reservoirs. The dashed arrows represent all other process fluxes with their associated N:P ratios. Dissolved reactive N:P ratios are given (N:P), together with the ratios of individual species. N:P ratios of fluxes entering and exiting WMDW and EMDW (bottom of figure) correspond to external sources and sinks to the DW.

removing accumulating refractory DOP and DON, whereas a similar mechanism does not operate in the EMS [*Rohling et al.*, 2015]. To exit the EMDW reservoir, refractory DOP and DON must first be transferred to the EMIW via upwelling before they can be transported out of the EMS via the Strait of Sicily.

3.5. N:P Ratios: WMS Versus EMS

Unusually high N:P ratios in all water column reservoirs are a defining feature of the EMS [*Krom et al.*, 2005] and, although somewhat less pronounced, also of the WMS [*Pujo-Pay et al.*, 2011]. While all reservoirs exhibit molar N:P ratios in excess of the Redfield ratio of 16:1, it is the NO_3:PO_4 ratios of the DW reservoirs that have received most attention. Measured NO_3:PO_4 ratios increase from around 20–23:1 in WMDW to 26–30:1 in EMDW [*Krom et al.*, 1991; *Béthoux et al.*, 1998; *Kress and Herut*, 2001; *Moutin and Raimbault*, 2002; *Ribera d'Alcalà et al.*, 2003; *Schroeder et al.*, 2010; *Pujo-Pay et al.*, 2011]. The very high EMDW NO_3:PO_4 ratio has previously been explained by the high N:P ratios of the combined external inputs to the EMS, along with negligible denitrification [*Krom et al.*, 2010; *Van Cappellen et al.*, 2014].

The molar N:P ratios of all 1950 model reservoirs and fluxes are summarized in Figures 6 and 7. Note that even before the large increases in anthropogenic P and N inputs that took place after 1950, the reactive N:P ratios of external inputs to the MS exceeded the Redfield ratio. In particular, the soluble reactive N:P ratios of atmospheric deposition and SGD are very high: 85–91:1 and 346–381:1, respectively (Figure 6). The ratio of the total reactive inputs into the WMS (30:1) is distinctly lower than for the EMS (37:1) (Figure 6), which helps explain the lower NO_3:PO_4 ratio of WMDW (21:1) compared to EMDW (28:1) (Figure 7). According to the DW NO_3:PO_4 sensitivity analyses (Figures 2g and 2i), the lower reactive N:P input ratio of the WMS is

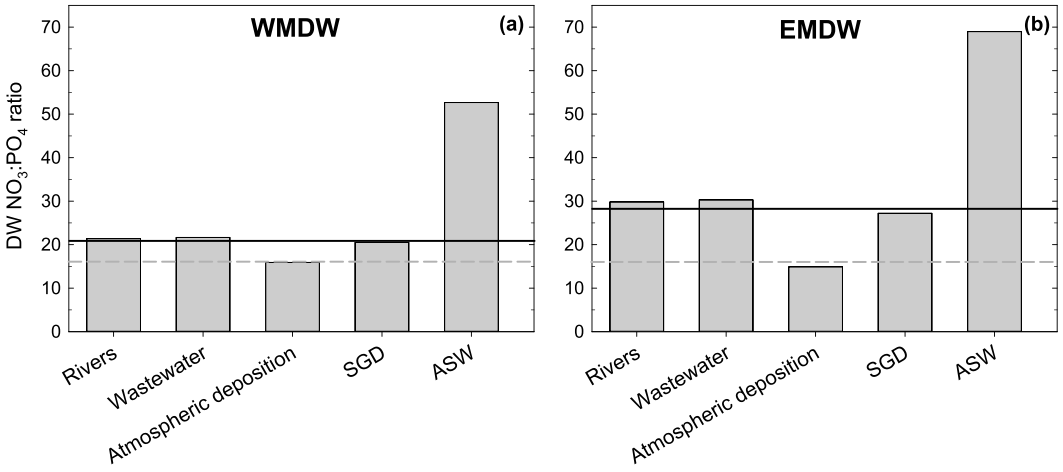

Figure 8. Response of the NO_3:PO_4 ratio in (a) WMDW and (b) EMDW after removing the stated individual input from the 1950 baseline simulation and running the model to its new steady state. The solid line represents the 1950 DW NO_3:PO_4 ratio, and the dashed line represents the Redfield ratio of 16:1. SGD = submarine groundwater discharge; ASW = Atlantic surface water input through the Strait of Gibraltar.

largely due to the low N:P ratio of the incoming ASW, which represents the main source of reactive P and N to the MS (see also *Lazzari et al.* [2016]).

The ASW flowing into the WMS is depleted in nitrate, with an estimated NO_3:PO_4 ratio of only 10:1 [*Coste et al.*, 1984; *Gómez et al.*, 2000; *Dafner et al.*, 2003; *Huertas et al.*, 2012]. Its dissolved reactive N:P ratio, however, is 21:1, because of the relatively high DON concentration of ASW (Figures 3 and 6). The high N:P of other external inputs to the WMS causes WMSW entering the EMS through the Strait of Sicily to be more P depleted, relative to N, than ASW entering through the Strait of Gibraltar. Our estimates yield a dissolved reactive N:P ratio of 30:1 for the SW flowing into the EMS from the WMS (Figure 6). Thus, the exchanges between the two basins of the MS are a key reason for the more extensive P limitation of the EMS, compared to the WMS. In addition, the greater recycling of DOP relative to DON in WMDW contributes to the lower NO_3:PO_4 ratio in the WMDW than EMDW (Figures 5 and 7).

Overall, the results summarized in Figures 6 and 7 align with the conclusions of *Krom et al.* [2010] and *Van Cappellen et al.* [2014], who proposed that the NO_3:PO_4 ratio in EMDW is a consequence of a very low denitrification rate in the EMS (0.002 mol N m^{-2} yr^{-1} or 2.4×10^9 mol N yr^{-1}), which preserves the signature of the high N:P ratios of the external nutrient sources, and the preferential recycling of P compared to N. In the EMS, field measurements further reveal an insignificant role of N_2 fixation in controlling water column NO_3:PO_4 ratios [*Ibello et al.*, 2010; *Bonnet et al.*, 2011; *Rahav et al.*, 2013]. Nitrogen fixation is therefore not considered in the EMS nutrient model.

Measurable N_2 fixation rates have been reported for the WMS, however [*Garcia et al.*, 2006; *Sandroni et al.*, 2007; *Ibello et al.*, 2010; *Bonnet et al.*, 2011]. While N_2 fixation could potentially help explain the relatively high NO_3:PO_4 ratio of WMDW, as previously proposed, our results suggest that this is not the case, because the estimated N_2 fixation (12.1×10^9 mol N yr^{-1}; Table 3 and Figure 3) is more than offset by the higher denitrification rate of the WMS (18×10^9 mol N yr^{-1} or 0.02 mol N m^{-2} yr^{-1}). The potential role of N_2 fixation and denitrification in controlling the WMDW NO_3:PO_4 ratio is also assessed by running the 1950 WMS-EMS model with no N_2 fixation and denitrification. Resulting DW NO_3:PO_4 ratios of 23.2 and 29.2 in the WMDW and EMDW, respectively, indicate that denitrification and N_2 fixation have minimal impacts on the unusual NO_3:PO_4 ratios within the MS, which is also in line with the sensitivity analyses (section 2.8 and Figure 2). We therefore conclude that similar to the EMS, the high NO_3:PO_4 ratio of the WMDW is also due to the high N:P ratio of the external non-marine nutrient sources and low denitrification rates in line with the trends presented by *Huertas et al.* [2012].

The relative impacts of the various external inputs on the NO_3:PO_4 ratios of WMDW and EMDW are illustrated in Figure 8, which shows the model-predicted ratios upon removing one nutrient source at a time. A key

observation is that when atmospheric deposition is excluded, the new steady state NO_3:PO_4 ratios of the WMS (16:1) and EMS (15:1) drop down to values close to the Redfield value. For the EMS, this is in agreement with *Christodoulaki et al.* [2013], who predict that if there were no atmospheric inputs to the EMS, the NO_3:PO_4 ratio of EMDW would approach the Redfield ratio. The relative supplies of P and N by atmospheric deposition are thus a major driver of the unusually high NO_3:PO_4 ratios that characterize the MS. The results in Figure 8 further indicate that riverine inputs, direct wastewater discharges, and SGD have little impact on the DW N:P ratios. However, in the absence of ASW inflow through the Strait of Gibraltar the NO_3:PO_4 ratios increase to 53 in the WMDW and 69 in the EMDW, confirming the important role of ASW inflow in buffering against even higher than observed DW NO_3:PO_4 ratios. Interestingly, the impact of ASW inflow through the Strait of Gibraltar on the DW NO_3:PO_4 ratios is greater for the EMS than the WMS.

Finally, the model results also demonstrate the importance of the low rates of denitrification in the MS compared to the global ocean [*Tyrrell*, 1999]. To bring the DW NO_3:PO_4 ratios down to the Redfield value of 16:1, the denitrification flux in the WMS would need to increase to 0.05 mol N m^{-2} yr^{-1} (i.e., 2.2 times greater than the 1950 flux) and in the EMS to 0.01 mol N m^{-2} yr^{-1} (i.e., 7 times greater than the 1950 flux). These values are comparable to rates in denitrification found in the global ocean (0.04–0.10 mol N m^{-2} yr^{-1} [*Codispoti*, 2007; *DeVries et al.*, 2012]). In other words, if the MS supported rates of denitrification similar to those generally observed in marine systems its NO_3:PO_4 ratios would fall along the global oceanic trend of 16:1.

4. Conclusions

The distinctive biogeochemical signatures of the MS are interpreted with the help of a mass balance model of the cycles of P and N. The model provides estimates of all the inputs of P and N to the MS in the mid-twentieth century, including those associated with the inflow of ASW through the Strait of Gibraltar and, for the first time, SGD and direct domestic wastewater discharges from coastal cities. It further accounts for the transformations among the different pools of P and N, vertical exchanges, including deepwater formation, upwelling and turbulent mixing, and lateral exchanges through the Straits of Gibraltar and Sicily.

The estimated model fluxes highlight the major role of the bidirectional flows through the Straits of Gibraltar and Sicily, which transport both dissolved inorganic and organic P and N in and out of the WMS and EMS. They further emphasize the importance of the cycling of organic P and organic N in the biogeochemical functioning of the MS. Inflow of ASW represents the main source of reactive P and N to the WMS, providing up to 60% of the total inputs, of which around half or more are in the form of DOP and DON. Similarly, inflow of SW from the WMS through the Strait of Sicily is the major source of reactive P and N to the EMS, providing up to 75% of the nutrient inputs. Primary productivity in the WMS is higher than in the EMS, primarily because the total inputs of marine-derived reactive P and N per unit surface area are 3 to 4 times higher for the WMS than the EMS. The surface-normalized non-marine (or land-derived) inputs of reactive P and N to the WMS and EMS, however, are of comparable magnitudes.

Inflow of ASW through the Strait of Gibraltar plus upwelling from WMIW to WMSW supports approximately 84% of new production in the WMS, consistent with the sensitivity analyses that indicate that primary productivity in the WMS is most sensitive to the inflow of ASW. In the EMS, the thermohaline circulation is dominated by downwelling resulting in 48% of new production supported by turbulent mixing from EMIW with an additional 37% sustained by the inflow of WMSW through the Strait of Sicily. The supply of DOP is a major source of new production, with 26% and 37% of the DOP supplied to WMSW and EMSW, respectively, remineralized and potentially used for new production.

The sensitivity analyses highlight the strong coupling of primary production in the EMS to processes occurring in the WMSW. In particular, uptake of PO_4 in the WMSW greatly reduces the proportion of PO_4 in the flux of dissolved reactive P supplied by the WMS to the EMS via the Strait of Sicily. Overall, the larger input of reactive P to the WMS explains the higher primary productivity in the WMS, which in turn supports greater bacterial activity and nutrient recycling in the WMS compared to the EMS. As a consequence, PO_4 and NO_3 concentrations are higher in the WMS than EMS, while DOP and DON concentrations are similar.

The MS acts as a bioreactor of organic nutrient cycling. In addition to the net delivery of DOP and DON from external sources, PO_4 and NO_3 are converted into organic matter in the SW. Downwelling transfers DOP and DON to the deeper layers, where mineralization turn DOP, and to a lesser extent DON, into PO_4 and NO_3. The

latter accumulate in the IW and DW and are exported through the Strait of Sicily and, ultimately, through the Strait of Gibraltar to the Atlantic Ocean. The anti-estuarine circulation thus not only maintains the MS in an oligotrophic state but also explains its net heterotrophy.

Lateral fluxes through the Straits of Gibraltar and Sicily and recycling of organic nutrients play key roles in determining the NO_3:PO_4 ratios of the WMDW and EMDW. Our results imply that the lower NO_3:PO_4 ratio of WMDW than EMDW is caused by the lower reactive N:P ratio of inputs into the WMS than EMS. The latter reflects the low NO_3:PO_4 ratio of ASW entering the WMS, together with faster recycling of DOP than DON within the WMDW. The high NO_3:PO_4 ratio of the entire MS is largely due to the high reactive N:P ratio of atmospheric deposition: without this input the WMDW and EMDW NO_3:PO_4 ratios would approach the Redfield value. Processes that regulate the NO_3:PO_4 ratio in the global ocean, in particular the balance between N_2 fixation and denitrification, are relatively unimportant in the MS. Finally, our analysis shows that the EMDW NO_3:PO_4 ratio is more sensitive than that of the WMDW ratio to changes of the internal and external models parameters. Thus, changes in the EMDW NO_3:PO_4 ratio could be a more sensitive indicator of changes in anthropogenic nutrient inputs than the changes in the WMDW ratio.

Although the coupled WMS-EMS model offers a simplified representation of the biogeochemical cycles of P and N, ignoring mesoscale variability and seasonality, it helps to identify the basin-scale biogeochemical and oceanographic processes that control P and N cycling in the MS on annual to decadal timescales. It also allows us to develop specific hypotheses that can guide the design of further studies on the MS. Based on the work presented here, we suggest that future research should concentrate on improving the quantification of the inputs, distributions, lability, and recycling of organic P and organic N across the MS. We strongly recommend the acquisition of internally comparable, multi-nutrient data in both the WMS and EMS. Particular attention should be given to the lateral fluxes of organic and inorganic P and N through the Straits of Gibraltar and Sicily, and the role of atmospheric deposition in the P and N cycles of the MS.

Acknowledgments
We thank Pere Masqué for providing the sediment core samples, Chris Parsons and Kassandra Ma for advice and assistance in analyzing the sediments, and Kay-Christian Emeis for useful discussions on biogeochemical cycling in the Mediterranean Sea. This work was funded by the Canada Excellence Research Chair (CERC) Program. All data for this paper are properly cited and referred to in the reference list and presented in figures and tables of this manuscript and supporting information. The source code for this study is available from the authors upon request (hrpowley@uwaterloo.ca).

References

Allen, J. I., P. J. Somerfield, and J. Siddorn (2002), Primary and bacterial production in the Mediterranean Sea: A modelling study, *J. Mar. Syst.*, *33*, 473–495, doi:10.1016/s0924-7963(02)00072-6.

Aminot, A., and R. Kérouel (2004), Dissolved organic carbon, nitrogen and phosphorus in the N-E Atlantic and the N-W Mediterranean with particular reference to non-refractory fractions and degradation, *Deep Sea Res., Part I*, *51*(12), 1975–1999, doi:10.1016/j.dsr.2004.07.016.

Arrigo, K. R. (2005), Marine microorganisms and global nutrient cycles, *Nature*, *437*(7057), 349–355, doi:10.1038/nature04158.

Asai, K., J. Zhang, K. Asai, K. Mogi, W. Y. Fantong, and A. K. Mandal (2013), Development of an in situ sampler of submarine springs for the analysis of CFCs and SF6, *Geochem. J.*, *47*(6), 693–696, doi:10.2343/geochemj.2.0253.

Aspila, K. I., H. Agemian, and A. S. Y. Chau (1976), Semi-automated method for determination of inorganic, organic and total phosphate in sediments, *Analyst*, *101*(1200), 187–197, doi:10.1039/an9760100187.

Banoub, M. W., and P. J. Williams (1972), Measuremnets of microbial activity and organic material in the western Mediterranean Sea, *Deep-Sea Res.*, *19*(6), 433–443, doi:10.1016/0011-7471(72)90053-8.

Bayari, C. S., N. N. Ozyurt, M. Oztan, Y. Bastanlar, G. Varinlioglu, H. Koyuncu, H. Ulkenli, and S. Hamarat (2011), Submarine and coastal karstic groundwater discharges along the southwestern Mediterranean coast of Turkey, *Hydrogeol. J.*, *19*(2), 399–414, doi:10.1007/s10040-010-0677-y.

Bergametti, G., E. Remoudaki, R. Losno, E. Steiner, B. Chatenet, and P. Buatmenard (1992), Source, transport and deposition of atmospheric phosphorus over the northwestern Mediterranean, *J. Atmos. Chem.*, *14*(1–4), 501–513, doi:10.1007/bf00115254.

Berman-Frank, I., and E. Rahav (2012), Dinitrogen fixation as a souce for new production in the Mediterranean Sea: A review, in *Life in the Mediterranean Sea: A Look at Habitat Changes*, edited by N. Stambler, pp. 199–226, Nova Sci. Publ., New York.

Béthoux, J. P. (1980), Mean water fluxes across sections in the Mediterranean Sea, evaluated on the basis of water and salt budgets and of observed salinities, *Oceanol. Acta*, *3*(1), 79–88.

Béthoux, J. P. (1989), Oxygen consumption, new production, vertical advection and environmental evolution in the Mediterranean Sea, *Deep Sea Res., Part A*, *36*(5), 769–781, doi:10.1016/0198-0149(89)90150-7.

Béthoux, J. P., P. Morin, C. Madec, and B. Gentili (1992), Phosphorus and nitrogen behavior in the Mediterranean Sea, *Deep-Sea Res., Part A*, *39*(9A), 1641–1654.

Béthoux, J. P., P. Morin, C. Chaumery, O. Connan, B. Gentili, and D. Ruiz-Pino (1998), Nutrients in the Mediterranean Sea, mass balance and statistical analysis of concentrations with respect to environmental change, *Mar. Chem.*, *63*(1–2), 155–169.

Béthoux, J. P., P. Morin, and D. P. Ruiz-Pino (2002), Temporal trends in nutrient ratios: Chemical evidence of Mediterranean ecosystem changes driven by human activity, *Deep Sea Res., Part II*, *49*(11), 2007–2016, doi:10.1016/s0967-0645(02)00024-3.

Béthoux, J. P., M. S. El Boukhary, D. Ruiz-Pino, P. Morin, and C. Copin-Montégut (2005), Nutrient, oxygen and carbon ratios, CO_2 sequestration and anthropogenic forcing in the Mediterranean Sea, in *The Mediterranean Sea*, *Handb. Environ. Chem.*, vol. 5K, edited by A. Saliot, pp. 67–86, Springer, Berlin, Heidelberg, doi:10.1007/b107144.

Bonnet, S., O. Grosso, and T. Moutin (2011), Planktonic dinitrogen fixation along a longitudinal gradient across the Mediterranean Sea during the stratified period (BOUM cruise), *Biogeosciences*, *8*(8), 2257–2267, doi:10.5194/bg-8-2257-2011.

Box, G. E. P., W. G. Hunter, and J. S. Hunter (1978), *Statistics for Experimenters. An Introduction to Design, Data Analysis and Model Building*, p. 653, John Wiley, New York.

Burnett, W. C., et al. (2006), Quantifying submarine groundwater discharge in the coastal zone via multiple methods, *Sci. Total Environ.*, *367*(2–3), 498–543, doi:10.1016/j.scitotenv.2006.05.009.
Burnett, W. C., G. Wattayakorn, M. Taniguchi, H. Dulaiova, P. Sojisuporn, S. Rungsupa, and T. Ishitobi (2007), Groundwater-derived nutrient inputs to the upper Gulf of Thailand, *Cont. Shelf Res.*, *27*(2), 176–190, doi:10.1016/j.csr.2006.09.006.
Charideh, A., and A. Rahman (2007), Environmental isotopic and hydrochemical study of water in the karst aquifer and submarine springs of the Syrian coast, *Hydrogeol. J.*, *15*(2), 351–364, doi:10.1007/s10040-006-0072-x.
Christodoulaki, S., G. Petihakis, M. Kanakidou, N. Mihalopoulos, K. Tsiaras, and G. Triantafyllou (2013), Atmospheric deposition in the eastern Mediterranean. A driving force for ecosystem dynamics, *J. Mar. Syst.*, *109*, 78–93, doi:10.1016/j.jmarsys.2012.07.007.
Codispoti, L. A. (2007), An oceanic fixed nitrogen sink exceeding 400 Tg N a^{-1} vs the concept of homeostasis in the fixed-nitrogen inventory, *Biogeosciences*, *4*(2), 233–253.
Copin-Montegut, C., and G. Copin-Montegut (1983), Stoichiometry of carbon, nitrogen, and phosphorus in marine particulate matter, *Deep-Sea Res., Part A*, *30*(1), 31–46, doi:10.1016/0198-0149(83)90031-6.
Coste, B., H. J. Minas, and M.-C. Bonin (1984), Propriétés hydrologiques et chimiques des eaux du bassin occidental de la Méditerranée. Campagne Medripod IV - 15 Octobre - 17 Novembre 1981, Rep., Centre natl. pour l'exploitation des océans, Brest CEDEX, France.
Coste, B., P. Lecorre, and H. J. Minas (1988), Reevaluation of the nutrient exchanges in the Strait of Gibralter, *Deep-Sea Res., Part A*, *35*(5), 767–775, doi:10.1016/0198-0149(88)90029-5.
Crispi, G., R. Mosetti, C. Solidoro, and A. Crise (2001), Nutrients cycling in Mediterranean basins: The role of the biological pump in the trophic regime, *Ecol. Model.*, *138*(1–3), 101–114, doi:10.1016/s0304-3800(00)00396-3.
Dafner, E., R. Boscolo, and H. L. Bryden (2003), The N: Si: P molar ratio in the strait of Gibraltar, *Geophys. Res. Lett.*, *30*(10), 1506, doi:10.1029/2002GL016274.
de Madron, X. D., et al. (2003), Nutrients and carbon budgets for the Gulf of Lion during the Moogli cruises, *Oceanol. Acta*, *26*(4), 421–433, doi:10.1016/s0399-1784(03)00024-0.
Denis, L., and C. Grenz (2003), Spatial variability in oxygen and nutrient fluxes at the sediment-water interface on the continental shelf in the Gulf of Lions (NW Mediterranean), *Oceanol. Acta*, *26*(4), 373–389, doi:10.1016/s0399-1784(03)00017-3.
Denis-Karafistan, A., J. M. Martin, H. Minas, P. Brasseur, J. Nihoul, and C. Denis (1998), Space and seasonal distributions of nitrates in the Mediterranean Sea derived from a variational inverse model, *Deep Sea Res., Part I*, *45*(2–3), 387–408, doi:10.1016/s0967-0637(97)00089-7.
DeVries, T., C. Deutsch, F. Primeau, B. Chang, and A. Devol (2012), Global rates of water-column denitrification derived from nitrogen gas measurements, *Nat. Geosci.*, *5*(8), 547–550, doi:10.1038/ngeo1515.
Diaz, F., and P. Raimbault (2000), Nitrogen regeneration and dissolved organic nitrogen release during spring in a NW Mediterranean coastal zone (Gulf of Lions): Implications for the estimation of new production, *Mar. Ecol. Prog. Ser.*, *197*, 51–65, doi:10.3354/meps197051.
Diaz, F., P. Raimbault, B. Boudjellal, N. Garcia, and T. Moutin (2001), Early spring phosphorus limitation of primary productivity in a NW Mediterranean coastal zone (Gulf of Lions), *Mar. Ecol. Prog. Ser.*, *211*, 51–62, doi:10.3354/meps211051.
Doval, M. D., F. F. Perez, and E. Berdalet (1999), Dissolved and particulate organic carbon and nitrogen in the northwestern Mediterranean, *Deep Sea Res., Part I*, *46*(3), 511–527, doi:10.1016/s0967-0637(98)00072-7.
Doval, M. D., X. A. Alvarez-Salgado, and F. F. Perez (2001), Organic matter distributions in the eastern North Atlantic-Azores Front region, *J. Mar. Syst.*, *30*(1–2), 33–49, doi:10.1016/s0924-7963(01)00036-7.
Dowling, C. B., R. J. Poreda, and A. R. Basu (2003), The groundwater geochemistry of the Bengal Basin: Weathering, chemsorption, and trace metal flux to the oceans, *Geochim. Cosmochim. Acta*, *67*(12), 2117–2136, doi:10.1016/s0016-7037(02)01306-6.
Duarte, C. M., M. Holmer, Y. Olsen, D. Soto, N. Marbà, J. Guiu, K. Black, and I. Karakassis (2009), Will the oceans help feed humanity?, *Bioscience*, *59*(11), 967–976, doi:10.1525/bio.2009.59.11.8.
Duarte, C. M., A. Regaudie-de-Gioux, J. M. Arrieta, A. Delgado-Huertas, and S. Agusti (2013), The Oligotrophic Ocean is heterotrophic, *Ann. Rev. Mar. Sci.*, *5*, 551–569.
El-Gamal, A. A., R. N. Peterson, and W. C. Burnett (2012), Detecting freshwater inputs via groundwater discharge to Marina Lagoon, Mediterranean Coast, Egypt, *Estuaries Coasts*, *35*(6), 1486–1499, doi:10.1007/s12237-012-9539-2.
Eppley, R. W., and B. J. Peterson (1979), Particulate organic-matter flux and planktonic new production in the deep ocean, *Nature*, *282*(5740), 677–680, doi:10.1038/282677a0.
Erisman, J. W., H. van Grinsven, B. Grizzetti, F. Bouraoui, D. Powlson, M. A. Sutton, A. Bleeker, and S. Reis (2011), The European nitrogen problem in a global perspective, in *The European Nitrogen Assessment*, edited by M. A. Sutton et al., pp. 9–31, Cambridge Univ. Press, Cambridge, U. K.
Falkowski, P., et al. (2000), The global carbon cycle: A test of our knowledge of Earth as a system, *Science*, *290*(5490), 291–296, doi:10.1126/science.290.5490.291.
FAOSTAT (2015a), Fertilizer consumption: Nitrogenous and phosphate fertilizers. [Available at http://faostat3.fao.org/download/R/RA/E, accessed 7/05/2016.]
FAOSTAT (2015b), Emissions agriculture: Manure management: Manure N content. [Available at http://faostat3.fao.org/download/G1/GM/E, accessed 12/05/16.]
FAOSTAT (2016), Annual population. [Available at http://faostat3.fao.org/download/O/OA/E, accessed 13/05/2016.]
Garcia, N., P. Raimbault, E. Gouze, and V. Sandroni (2006), Nitrogen fixation and primary production in western Mediterranean, *C. R. Biol.*, *329*(9), 742–750, doi:10.1016/j.crvi.2006.06.006.
Garcia-Solsona, E., J. Garcia-Orellana, P. Masque, V. Rodellas, M. Mejias, B. Ballesteros, and J. A. Dominguez (2010), Groundwater and nutrient discharge through karstic coastal springs (Castello, Spain), *Biogeosciences*, *7*(9), 2625–2638, doi:10.5194/bg-7-2625-2010.
Gehlen, M., C. Rabouille, U. Ezat, and L. D. GuidiGuilvard (1997), Drastic changes in deep-sea sediment porewater composition induced by episodic input of organic matter, *Limnol. Oceanogr.*, *42*(5), 980–986.
Geider, R. J., and J. La Roche (2002), Redfield revisited: Variability of C: N: P in marine microalgae and its biochemical basis, *Eur. J. Phycol.*, *37*(1), 1–17, doi:10.1017/s0967026201003456.
Gómez, F., N. González, F. Echevarria, and C. M. Garcia (2000), Distribution and fluxes of dissolved nutrients in the Strait of Gibraltar and its relationships to microphytoplankton biomass, *Estuarine Coastal Shelf. Sci.*, *51*(4), 439–449, doi:10.1006/ecss.2000.0689.
Guerzoni, S., et al. (1999), The role of atmospheric deposition in the biogeochemistry of the Mediterranean Sea, *Prog. Oceanogr.*, *44*(1–3), 147–190.
Heimbürger, L.-E., D. Cossa, B. Thibodeau, A. Khripounoff, V. Mas, J.-F. Chiffoleau, S. Schmidt, and C. Migon (2012), Natural and anthropogenic trace metals in sediments of the Ligurian Sea (northwestern Mediterranean), *Chem. Geol.*, *291*, 141–151, doi:10.1016/j.chemgeo.2011.10.011.

Huertas, I. E., A. F. Ríos, J. García-Lafuente, G. Navarro, A. Makaoui, A. Sánchez-Román, S. Rodriguez-Galvez, A. Orbi, J. Ruíz, and F. F. Pérez (2012), Atlantic forcing of the Mediterranean oligotrophy, *Global Biogeochem. Cycles*, *26*, GB2022, doi:10.1029/2011GB004167.

Ibello, V., C. Cantoni, S. Cozzi, and G. Civitarese (2010), First basin-wide experimental results on N_2 fixation in the open Mediterranean Sea, *Geophys. Res. Lett.*, *37*, L03608, doi:10.1029/2009GL041635.

Karafistan, A., J. M. Martin, M. Rixen, and J. M. Beckers (2002), Space and time distributions of phosphate in the Mediterranean Sea, *Deep Sea Res., Part I*, *49*(1), 67–82.

Kim, T.-H., E. Kwon, I. Kim, S.-A. Lee, and G. Kim (2013), Dissolved organic matter in the subterranean estuary of a volcanic island, Jeju: Importance of dissolved organic nitrogen fluxes to the ocean, *J. Sea Res.*, *78*, 18–24, doi:10.1016/j.seares.2012.12.009.

Klausmeier, C. A., E. Litchman, T. Daufresne, and S. A. Levin (2004), Optimal nitrogen-to-phosphorus stoichiometry of phytoplankton, *Nature*, *429*(6988), 171–174, doi:10.1038/nature02454.

Kouvarakis, G., N. Mihalopoulos, A. Tselepides, and S. Stavrakakis (2001), On the importance of atmospheric inputs of inorganic nitrogen species on the productivity of the eastern Mediterranean Sea, *Global Biogeochem. Cycles*, *15*(4), 805–817, doi:10.1029/2001GB001399.

Kress, N., and B. Herut (2001), Spatial and seasonal evolution of dissolved oxygen and nutrients in the southern Levantine Basin (eastern Mediterranean Sea): Chemical characterization of the water masses and inferences on the N:P ratios, *Deep Sea Res., Part I*, *48*(11), 2347–2372.

Kroeger, K. D., P. W. Swarzenski, W. J. Greenwood, and C. Reich (2007), Submarine groundwater discharge to Tampa Bay: Nutrient fluxes and biogeochemistry of the coastal aquifer, *Mar. Chem.*, *104*(1–2), 85–97, doi:10.1016/j.marchem.2006.10.012.

Krom, M. D., N. Kress, S. Brenner, and L. I. Gordon (1991), Phosphorus limitation of primary productivity in the eastern Mediterranean, *Limnol. Oceanogr.*, *36*(3), 424–432.

Krom, M. D., S. Brenner, N. Kress, A. Neori, and L. I. Gordon (1992), Nutrient dynamics and new production in a warm-core eddy from the eastern Mediterranean, *Deep-Sea Res., Part A*, *39*(3-4A), 467–480, doi:10.1016/0198-0149(92)90083-6.

Krom, M. D., et al. (2005), Nutrient cycling in the south east Levantine basin of the eastern Mediterranean: Results from a phosphorus starved system, *Deep Sea Res., Part II*, *52*(22–23), 2879–2896, doi:10.1016/j.dsr.2005.08.009.

Krom, M. D., K. C. Emeis, and P. Van Cappellen (2010), Why is the eastern Mediterranean phosphorus limited?, *Prog. Oceanogr.*, *85*(3–4), 236–244, doi:10.1016/j.pocean.2010.03.003.

Krom, M. D., N. Kress, I. Berman-Frank, and E. Rahav (2014), Past, present and future patterns in the nutrient chemistry of the eastern Mediterranean, in *The Mediterranean Sea. Its History and Present Challenges*, edited by S. Goffredo and Z. Dubinsky, pp. 49–68, Springer, Dordrecht, Netherlands.

L'Helguen, S., P. Le Corre, C. Madec, and P. Morin (2002), New and regenerated production in the Almeria-Oran front area, eastern Alboran Sea, *Deep Sea Res., Part I*, *49*(1), 83–99, doi:10.1016/s0967-0637(01)00044-9.

La Corre, P., P. Morin, and J.-L. Birrien (1984), Repartition de la matiere organique dissoute (N et P dissous), in *Propriétés Hydrologiques et Chimiques des Eaux du Bassin Occidental de la Méditerranée. Campagne Medripod IV - 15 Octobre - 17 Novembre 1981*, edited by B. Coste, H. J. Minas, and M.-C. Bonin, pp. 95–96, Centre National pour l'exploitation des Océans, Brest CEDEX, France.

Lazzari, P., C. Solidoro, V. Ibello, S. Salon, A. Teruzzi, K. Béranger, S. Colella, and A. Crise (2012), Seasonal and inter-annual variability of plankton chlorophyll and primary production in the Mediterranean Sea: A modelling approach, *Biogeosciences*, *9*(1), 217–233, doi:10.5194/bg-9-217-2012.

Lazzari, P., C. Solidoro, S. Salon, and G. Bolzon (2016), Spatial variability of phosphate and nitrate in the Mediterranean Sea: A modeling approach, *Deep Sea Res., Part I*, *108*, 39–52, doi:10.1016/j.dsr.2015.12.006.

LeBolloch, O., and S. Guerzoni (1995), Acid and alkaline deposition in precipitation on the western coast of Sardinia, Central Mediterranean (40°N, 8°E), *Water, Air, Soil Pollut.*, *85*(4), 2155–2160.

Letscher, R. T., F. Primeau, and J. K. Moore (2016), Nutrient budgets in the subtropical ocean gyres dominated by lateral transport, *Nat. Geosci.*, *9*(11), 815–819, doi:10.1038/ngeo2812.

Loÿe-Pilot, M. D., J. M. Martin, and J. Morelli (1990), Atmospheric input of inorganic nitrogen to the western Mediterranean, *Biogeochemistry*, *9*(2), 117–134, doi:10.1007/bf00692168.

Lucea, A., C. M. Duarte, S. Agusti, and M. Sondergaard (2003), Nutrient (N, P and Si) and carbon partitioning in the stratified NW Mediterranean, *J. Sea Res.*, *49*(3), 157–170, doi:10.1016/s1385-1101(03)00005-4.

Ludwig, W., E. Dumont, M. Meybeck, and S. Heussner (2009), River discharges of water and nutrients to the Mediterranean and Black Sea: Major drivers for ecosystem changes during past and future decades?, *Prog. Oceanogr.*, *80*(3–4), 199–217, doi:10.1016/j.pocean.2009.02.001.

Ludwig, W., A. F. Bouwman, E. Dumont, and F. Lespinas (2010), Water and nutrient fluxes from major Mediterranean and Black Sea rivers: Past and future trends and their implications for the basin-scale budgets, *Global Biogeochem. Cycles*, *24*, GB0A13, doi:10.1029/2009GB003594.

Luna, G. M., S. Bianchelli, F. Decembrini, E. De Domenico, R. Danovaro, and A. Dell'Anno (2012), The dark portion of the Mediterranean Sea is a bioreactor of organic matter cycling, *Global Biogeochem. Cycles*, *26*, GB2017, doi:10.1029/2011GB004168.

Macias, D., E. Garcia-Gorriz, C. Piroddi, and A. Stips (2014), Biogeochemical control of marine productivity in the Mediterranean Sea during the last 50 years, *Global Biogeochem. Cycles*, *28*, 897–907, doi:10.1002/2014GB004846.

Macias, D., et al. (2007), Analysis of mixing and biogeochemical effects induced by tides on the Atlantic–Mediterranean flow in the Strait of Gibraltar through a physical–biological coupled model, *Prog. Oceanogr.*, *74*(2–3), 252–272, doi:10.1016/j.pocean.2007.04.006.

Makings, U., I. R. Santos, D. T. Maher, L. Golsby-Smith, and B. D. Eyre (2014), Importance of budgets for estimating the input of groundwater-derived nutrients to an eutrophic tidal river and estuary, *Estuarine, Coastal Shelf Sci.*, *143*, 65–76, doi:10.1016/j.ecss.2014.02.003.

Markaki, Z., M. D. Loÿe-Pilot, K. Violaki, L. Benyahya, and N. Mihalopoulos (2010), Variability of atmospheric deposition of dissolved nitrogen and phosphorus in the Mediterranean and possible link to the anomalous seawater N/P ratio, *Mar. Chem.*, *120*(1–4), 187–194, doi:10.1016/j.marchem.2008.10.005.

Marty, J. C., J. Chiaverini, M. D. Pizay, and B. Avril (2002), Seasonal and interannual dynamics of nutrients and phytoplankton pigments in the western Mediterranean Sea at the DYFAMED time-series station (1991–1999), *Deep Sea Res., Part II*, *49*(11), 1965–1985, doi:10.1016/s0967-0645(02)00022-x.

Marty, J. C., M. Goutx, C. Guigue, N. Leblond, and P. Raimbault (2009), Short-term changes in particulate fluxes measured by drifting sediment traps during end summer oligotrophic regime in the NW Mediterranean Sea, *Biogeosciences*, *6*(5), 887–899.

Masqué, P., J. Fabres, M. Canals, J. A. Sanchez-Cabeza, A. Sanchez-Vidal, I. Cacho, A. M. Calafat, and J. M. Bruach (2003), Accumulation rates of major constituents of hemipelagic sediments in the deep Alboran Sea: A centennial perspective of sedimentary dynamics, *Mar. Geol.*, *193*(3–4), 207–233, doi:10.1016/s0025-3227(02)00593-5.

McCarthy, J. J., C. Garside, J. L. Nevins, and R. T. Barber (1996), New production along 140 degrees W in the equatorial Pacific during and following the 1992 El Niño event, *Deep Sea Res., Part II*, *43*(4–6), 1065–1093, doi:10.1016/0967-0645(96)00022-7.

McGill, D. A. (1961), A preliminary study of oxygen and phosphate distribution in the Mediterranean Sea, *Deep-Sea Res.*, *8*(3–4), 259–269, doi:10.1016/0146-6313(61)90027-2.
Migon, C., and V. Sandroni (1999), Phosphorus in rainwater: Partitioning inputs and impact on the surface coastal ocean, *Limnol. Oceanogr.*, *44*(4), 1160–1165.
Migon, C., G. Copinmontegut, L. Elegant, and J. Morelli (1989), Atmospheirc input of nutrients to the coastal mediterranean area - biogeochemical implications, *Oceanol. Acta*, *12*(2), 187–191.
Migon, C., V. Sandroni, and J. P. Béthoux (2001), Atmospheric input of anthropogenic phosphorus to the northwest Mediterranean under oligotrophic conditions, *Mar. Environ. Res.*, *52*(5), 413–426, doi:10.1016/s0141-1136(01)00095-2.
Millero, F. J., D. Means, and C. Miller (1978), Densities of Mediterranean Sea waters, *Deep-Sea Res.*, *25*(6), 563–569, doi:10.1016/0146-6291(78)90644-6.
Mongin, M., D. M. Nelson, P. Pondaven, M. A. Brzezinski, and P. Treguer (2003), Simulation of upper-ocean biogeochemistry with a flexible-composition phytoplankton model: C, N and Si cycling in the western Sargasso Sea, *Deep Sea Res., Part I*, *50*(12), 1445–1480, doi:10.1016/j.dsr.2003.08.003.
Moutin, T., and P. Raimbault (2002), Primary production, carbon export and nutrients availability in western and eastern Mediterranean Sea in early summer 1996 (MINOS cruise), *J. Mar. Syst.*, *33*, 273–288, doi:10.1016/s0924-7963(02)00062-3.
Nenes, A., M. D. Krom, N. Mihalopoulos, P. Van Cappellen, Z. Shi, A. Bougiatioti, P. Zarmpas, and B. Herut (2011), Atmospheric acidification of mineral aerosols: A source of bioavailable phosphorus for the oceans, *Atmos. Chem. Phys.*, *11*(13), 6265–6272, doi:10.5194/acp-11-6265-2011.
Pasqueron de Fommervault, O., C. Migon, F. D'Ortenzio, M. Ribera d'Alcalà, and L. Coppola (2015), Temporal variability of nutrient concentrations in the northwestern Mediterranean sea (DYFAMED time-series station), *Deep Sea Res., Part I*, *100*, 1–12, doi:10.1016/j.dsr.2015.02.006.
Pinhassi, J., L. Gomez-Consarnau, L. Alonso-Saez, M. M. Sala, M. Vidal, C. Pedros-Alio, and J. M. Gasol (2006), Seasonal changes in bacterio-plankton nutrient limitation and their effects on bacterial community composition in the NW Mediterranean Sea, *Aquat. Microb. Ecol.*, *44*(3), 241–252, doi:10.3354/ame044241.
Powley, H. R., M. D. Krom, K.-C. Emeis, and P. Van Cappellen (2014), A biogeochemical model for phosphorus and nitrogen cycling in the eastern Mediterranean Sea (EMS). Part 2. Response of nutrient cycles and primary production to anthropogenic forcing: 1950–2000, *J. Mar. Syst.*, *139*, 420–432.
Powley, H. R., H. H. Dürr, A. T. Lima, M. D. Krom, and P. Van Cappellen (2016a), Direct discharges of domestic wastewater are a major source of phosphorus and nitrogen to the Mediterranean Sea, *Environ. Sci. Technol.*, *50*, 8722–8730, doi:10.1021/acs.est.6b01742.
Powley, H. R., M. D. Krom, and P. Van Cappellen (2016b), Circulation and oxygen cycling in the Mediterranean Sea: Sensitivity to future climate change, *J. Geophys. Res. Oceans*, *121*, 8230–8247, doi:10.1002/2016JC012224.
Pujo-Pay, M., P. Conan, and P. Raimbault (1995), Particulate and dissolved organic nitrogen and phosphorus in the north western Mediterranean Sea (EROS Discovery Cruise 1993), in *EROS 2000. (Europrean River Ocean System). Fifth Workhop on the North-West Mediterranean Sea. Water Pollution Research Report 32*, edited by J.-M. Martin and H. Barth, pp. 79–86, European Commission, Luxembourg.
Pujo-Pay, M., P. Conan, L. Oriol, V. Cornet-Barthaux, C. Falco, J. F. Ghiglione, C. Goyet, T. Moutin, and L. Prieur (2011), Integrated survey of elemental stoichiometry (C, N, P) from the western to eastern Mediterranean Sea, *Biogeosciences*, *8*(4), 883–899, doi:10.5194/bg-8-883-2011.
Rahav, E., B. Herut, N. Stambler, E. Bar-Zeev, M. R. Mulholland, and I. Berman-Frank (2013), Uncoupling between dinitrogen fixation and primary productivity in the eastern Mediterranean Sea, *J. Geophys. Res. Biogeosci.*, *118*, 195–202, doi:10.1002/jgrg.20023.
Ramirez, T., D. Cortes, J. M. Mercado, M. Vargas-Yanez, M. Sebastian, and E. Liger (2005), Seasonal dynamics of inorganic nutrients and phytoplankton biomass in the NW Alboran Sea, *Estuar. Coast. Shelf Sci.*, *65*(4), 654–670, doi:10.1016/j.ecss.2005.07.012.
Ramirez-Romero, E., D. Macias, C. M. Garcia, and M. Bruno (2014), Biogeochemical patterns in the Atlantic inflow through the Strait of Gibraltar, *Deep Sea Res., Part I*, *85*, 88–100, doi:10.1016/j.dsr.2013.12.004.
Redfield, A. C., B. H. Ketchum, and F. A. Richards (1963), The influence of organisms on the composition of seawater, in *The Sea*, edited by M. N. Hill, pp. 26–77, Interscience, New York.
Ribera d'Alcalà, M., G. Civitarese, F. Conversano, and R. Lavezza (2003), Nutrient ratios and fluxes hint at overlooked processes in the Mediterranean Sea, *J. Geophys. Res.*, *108*(C9), 8106, doi:10.1029/2002JC001650.
Ribera d'Alcala, M., C. Brunet, F. Conversano, F. Corato, and R. Lavezza (2009), Nutrient and pigment distributions in the southern Tyrrhenian Sea during mid-summer and late fall 2005, *Deep Sea Res., Part II*, *56*(11–12), 676–686, doi:10.1016/j.dsr2.2008.07.028.
Rodellas, V., J. Garcia-Orellana, P. Masque, M. Feldman, and Y. Weinstein (2015), Submarine groundwater discharge as a major source of nutrients to the Mediterranean Sea, *Proc. Natl. Acad. Sci. U.S.A.*, *112*(13), 3926–3930, doi:10.1073/pnas.1419049112.
Rohling, E. J., G. Marino, and K. M. Grant (2015), Mediterranean climate and oceanography, and the periodic development of anoxic events (sapropels), *Earth Sci. Rev.*, *143*, 62–97, doi:10.1016/j.earscirev.2015.01.008.
Ruttenberg, K. C., N. O. Ogawa, F. Tamburini, R. A. Briggs, N. D. Colasacco, and E. Joyce (2009), Improved, high-throughput approach for phosphorus speciation in natural sediments via the SEDEX sequential extraction method, *Limnol. Oceanogr. Methods*, *7*, 319–333.
Sanchez-Cabeza, J. A., P. Masque, I. Ani-Ragolta, J. Merino, M. Frignani, F. Alvisi, A. Palanques, and P. Puig (1999), Sediment accumulation rates in the southern Barcelona continental margin (NW Mediterranean Sea) derived from Pb-210 and Cs-137 chronology, *Prog. Oceanogr.*, *44*(1–3), 313–332, doi:10.1016/s0079-6611(99)00031-2.
Sandroni, V., P. Raimbault, C. Migon, N. Garcia, and E. Gouze (2007), Dry atmospheric deposition and diazotrophy as sources of new nitrogen to northwestern Mediterranean oligotrophic surface waters, *Deep Sea Res., Part I*, *54*(11), 1859–1870, doi:10.1016/j.dsr.2007.08.004.
Santos, I. R., W. C. Burnett, T. Dittmar, I. G. N. A. Suryaputra, and J. Chanton (2009), Tidal pumping drives nutrient and dissolved organic matter dynamics in a Gulf of Mexico subterranean estuary, *Geochim. Cosmochim. Acta*, *73*(5), 1325–1339, doi:10.1016/j.gca.2008.11.029.
Santos, I. R., J. de Weys, D. R. Tait, and B. D. Eyre (2013), The contribution of groundwater discharge to nutrient exports from a coastal catchment: Post-flood seepage increases estuarine N/P ratios, *Estuaries Coasts*, *36*(1), 56–73, doi:10.1007/s12237-012-9561-4.
Schroeder, K., G. P. Gasparini, M. Borghini, G. Cerrati, and R. Delfanti (2010), Biogeochemical tracers and fluxes in the western Mediterranean Sea, spring 2005, *J. Mar. Syst.*, *80*(1–2), 8–24, doi:10.1016/j.jmarsys.2009.08.002.
Schroeder, K., et al. (2012), Circulation of the Mediterranean Sea and its variability, in *The Climate of the Mediterranean Region, from the Past to the Future*, edited by P. Lionello, pp. 187–256, Elsevier Insights, Amsterdam.
Severin, T., P. Conan, X. D. de Madron, L. Houpert, M. J. Oliver, L. Oriol, J. Caparros, J. F. Ghiglione, and M. Pujo-Pay (2014), Impact of open-ocean convection on nutrients, phytoplankton biomass and activity, *Deep Sea Res., Part I*, *94*, 62–71, doi:10.1016/j.dsr.2014.07.015.
Stockdale, A., M. D. Krom, R. J. G. Mortimer, L. G. Benning, K. S. Carslaw, R. J. Herbert, Z. B. Shi, S. Myriokefalitakis, M. Kanakidou, and A. Nenes (2016), Understanding the nature of atmospheric acid processing of mineral dusts in supplying bioavailable phosphorus to the oceans, *Proc. Natl. Acad. Sci. U.S.A.*, *113*(51), 14639–14644, doi:10.1073/pnas.1608136113.

Tait, D. R., D. V. Erler, I. R. Santos, T. J. Cyronak, U. Morgenstern, and B. D. Eyre (2014), The influence of groundwater inputs and age on nutrient dynamics in a coral reef lagoon, *Mar. Chem.*, *166*, 36–47, doi:10.1016/j.marchem.2014.08.004.

Tanhua, T., D. Hainbucher, V. Cardin, M. Alvarez, G. Civitarese, A. P. McNichol, and R. M. Key (2013), Repeat hydrography in the Mediterranean Sea, data from the Meteor cruise 84/3 in 2011, *Earth Syst. Sci. Data*, *5*(2), 289–294, doi:10.5194/essd-5-289-2013.

Thingstad, T. F., and F. Rassoulzadegan (1995), Nutrient limitations, microbial food webs and biological C-pumps—Suggested interactions in a P limited Mediterranean, *Mar. Ecol. Prog. Ser.*, *117*(1–3), 299–306, doi:10.3354/meps117299.

Thingstad, T. F., U. L. Zweifel, and F. Rassoulzadegan (1998), P limitation of heterotrophic bacteria and phytoplankton in the northwest Mediterranean, *Limnol. Oceanogr.*, *43*(1), 88–94.

Thingstad, T. F., et al. (2005), Nature of phosphorus limitation in the ultraoligotrophic eastern Mediterranean, *Science*, *309*(5737), 1068–1071, doi:10.1126/science.1112632.

Tovar-Sanchez, A., G. Basterretxea, V. Rodellas, D. Sanchez-Quiles, J. Garcia-Orellana, P. Masque, A. Jordi, J. M. Lopez, and E. Garcia-Solsona (2014), Contribution of groundwater discharge to the coastal dissolved nutrients and trace metal concentrations in Majorca Island: Karstic vs detrital systems, *Environ. Sci. Technol.*, *48*(20), 11819–11827, doi:10.1021/es502958t.

Turley, C. M., M. Bianchi, U. Christaki, P. Conan, J. R. W. Harris, S. Psarra, G. Ruddy, E. D. Stutt, A. Tselepides, and F. Van Wambeke (2000), Relationship between primary producers and bacteria in an oligotrophic sea—The Mediterranean and biogeochemical implications, *Mar. Ecol. Prog. Ser.*, *193*, 11–18, doi:10.3354/meps193011.

Tyrrell, T. (1999), The relative influences of nitrogen and phosphorus on oceanic primary production, *Nature*, *400*(6744), 525–531, doi:10.1038/22941.

Van Cappellen, P., H. R. Powley, K.-C. Emeis, and M. D. Krom (2014), A biogeochemical model for phosphorus and nitrogen cycling in the eastern Mediterranean Sea (EMS). Part 1. Model development, initial conditions and sensitivity analyses, *J. Mar. Syst.*, *139*, 460–471.

Van Den Broeck, N., and T. Moutin (2002), Phosphate in the sediments of the Gulf of Lions (NW Mediterranean Sea), relationship with input by the river Rhone, *Hydrobiologia*, *472*(1–3), 85–94, doi:10.1023/a:1016308931115.

Van Wambeke, F., U. Christaki, A. Giannokourou, T. Moutin, and K. Souvemerzoglou (2002), Longitudinal and vertical trends of bacterial limitation by phosphorus and carbon in the Mediterranean Sea, *Microb. Ecol.*, *43*(1), 119–133, doi:10.1007/s00248-001-0038-4.

Weinstein, Y., Y. Yechieli, Y. Shalem, W. C. Burnett, P. W. Swarzenski, and B. Herut (2011), What is the role of fresh groundwater and recirculated seawater in conveying nutrients to the coastal ocean?, *Environ. Sci. Technol.*, *45*(12), 5195–5200, doi:10.1021/es104394r.

Williams, P. J. L., P. D. Quay, T. K. Westberry, and M. J. Behrenfeld (2013), The oligotrophic ocean is autotrophic, *Ann. Rev. Mar. Sci.*, 5, 535–549.

Zaccone, R., A. Boldrin, G. Caruso, R. La Ferla, G. Maimone, C. Santinelli, and M. Turchetto (2012), Enzymatic activities and prokaryotic abundance in relation to organic matter along a Eest-East Mediterranean Transect (TRANSMED cruise), *Microb. Ecol.*, *64*(1), 54–66, doi:10.1007/s00248-012-0011-4.

Zekster, I. S., R. G. Dzhamalov, and L. G. Everett (2007), *Submarine Groundwater*, p. 466, Taylor and Francis Group, Fla.

Zohary, T., and R. D. Robarts (1998), Experimental study of microbial P limitation in the eastern Mediterranean, *Limnol. Oceanogr.*, *43*(3), 387–395.

Zúñiga, D., A. Calafat, A. Sanchez-Vidal, M. Canals, B. Price, S. Heussner, and S. Miserocchi (2007a), Particulate organic carbon budget in the open Algero-Balearic Basin (western Mediterranean): Assessment from a one-year sediment trap experiment, *Deep Sea Res., Part I*, *54*(9), 1530–1548, doi:10.1016/j.dsr.2007.06.001.

Zúñiga, D., J. García-Orellana, A. Calafat, N. B. Price, T. Adatte, A. Sanchez-Vidal, M. Canals, J. A. Sanchez-Cabeza, P. Masqué, and J. Fabres (2007b), Late Holocene fine-grained sediments of the Balearic Abyssal Plain, western Mediterranean Sea, *Mar. Geol.*, *237*(1–2), 25–36, doi:10.1016/j.margeo.2006.10.034.

Zúñiga, D., et al. (2008), Compositional and temporal evolution of particle fluxes in the open Algero–Balearic basin (western Mediterranean), *J. Mar. Syst.*, *70*(1–2), 196–214, doi:10.1016/j.jmarsys.2007.05.007.